SRC HOMOLOGY 2 DOMAIN-CONTAINING INOSITOL-5' PHOSPHATASE IN A MURINE MODEL OF AMYOTROPHIC LATERAL SCLEROSIS

by

Heather Parrott
Bachelor of Kinesiology, University of the Fraser Valley, 2006

THESIS SUBMITTED IN PARTIAL FULFILLMENT OF
THE REQUIREMENTS FOR THE DEGREE OF

MASTER OF SCIENCE

In the
Department of Biomedical Physiology and Kinesiology

SIMON FRASER UNIVERSITY

Summer, 2009

APPROVAL

Name: **Heather Parrott**

Degree: **Master of Science**

Title of Thesis: **Src homology 2 domain-containing inositol-5' phosphatase in a murine model of Amyotrophic Lateral Sclerosis**

Examining Committee:

Chair: **Dr. Steven Robinovitch**
Associate Professor– School of Biomedical Physiology and Kinesiology

_____

Dr. Charles Krieger
Senior Supervisor
Professor– School of Biomedical Physiology and Kinesiology

_____

Dr. Peter Ruben
Supervisor
Professor and Director – School of Biomedical Physiology and Kinesiology

_____

Dr. Neil Watson
External Examiner
Professor– Department of Psychology

Date Defended/Approved: 13-July-2009

Declaration of
Partial Copyright Licence

SFU SIMON FRASER UNIVERSITY
THINKING OF THE WORLD

STATEMENT OF ETHICS APPROVAL

The author, whose name appears on the title page of this work, has obtained, for the research described in this work, either:

(a) Human research ethics approval from the Simon Fraser University Office of Research Ethics,

or

(b) Advance approval of the animal care protocol from the University Animal Care Committee of Simon Fraser University;

or has conducted the research

(c) as a co-investigator, collaborator or research assistant in a research project approved in advance,

or

(d) as a member of a course approved in advance for minimal risk human research, by the Office of Research Ethics.

A copy of the approval letter has been filed at the Theses Office of the University Library at the time of submission of this thesis or project.

The original application for approval and letter of approval are filed with the relevant offices. Inquiries may be directed to those authorities.

Simon Fraser University Library
Simon Fraser University
Burnaby, BC, Canada

Last update: Spring 2010

ABSTRACT

As Src homology-2 domain-containing inositol-5' phosphatase (SHIP-1) expression has been implicated in inflammation, immunoreactivity against SHIP-1 was evaluated in mice over-expressing mutant superoxide dismutase (mSOD-1) and wild-type (wt) mice. Spinal cord sections were examined at 11 weeks, 15 weeks of age and at end-stage. SHIP-1 immunoreactivity was detected in mSOD-1 mice at end-stage when considerable motor disability is evident, and at 15 weeks, but not in wt mice. At 15 weeks, SHIP-1 was prominent in the ventral horn, and by end-stage, immunoreactivity was detected throughout the ventral and dorsal regions. SHIP-1 localization was explored further using SHIP-1 immunoreactivity and antibodies directed against microglia and astrocytes. SHIP-1 was not detected in microglia but was detected in astrocytes and this cell specific localization of immunoreactivity suggests that astrocytes can express SHIP-1. The expression of SHIP-1 in astrocytes may be involved in the pathogenesis of murine amyotrophic lateral sclerosis.

ACKNOWLEDGEMENTS

I would like to thank my senior supervisor, Dr. Charles Krieger, for welcoming into his laboratory and offering me an opportunity to challenge myself through the undertaking of this project, and for this continual support during my research. I would also like to thank Dr. Peter Ruben, for the guidance and he has offered me throughout the course of my graduate work at SFU.

Of note, I am extremely grateful for the skills and knowledge I have taken away from my research experience. I owe great thanks to Coral Lewis for her willingness to teach me numerous laboratory procedures, and for the dedicated effort she demonstrated through all levels of the project. I would also like to acknowledge Amy Tsai and Xiao Yang Shan for their assistance throughout the course of my research.

To my family and to the friends who helped me stay on path, I am truly thankful for your love, support and daily encouragement.

TABLE OF CONTENTS

LIST OF FIGURES

LIST OF TABLES

GLOSSARY

ALS	Amyotrophic lateral sclerosis
ArgI	Arginase-1
BAD	Bcl-2/Bcl-xL antagonist causing cell death
Bcl-2/Bcl-xL	B cell lymphoma 2
BCR	B cell receptor
BH	Break-point cluster homology
BSA	Bovine serum albumin
Btk	Bruton's tyrosine kinase
CD11b	Cluster of differentiation molecule 11B
Cdc42	Cell division cycle 42
CDK	Cyclin-dependent kinase
CNS	Central nervous system
Cy3	Cyanine 3
ERK	Extracellular signal-related protein kinase
FALS	Familial form of amyotrophic lateral sclerosis
FcR	Fc gamma receptor
FKHR	Forkhead transcription factor
FITC	Fluorescein isothiocyanate
Gab	Grb2 associated binder

GEF	Guanine exchange factors
GFAP	Glial fibrillary acidic protein
GMCSF	Granulocyte macrophage colony stimulating factor
Grb2	Growth protein receptor-bound protein 2
GSK3	Glycogen synthase kinase 3
GTP	Guanosine 5-trisphosphate
Iba-1	Ionized calcium binding adaptor 1
IFN	Interferon
Ig	Immunoglobulin
IHC	Immunohistochemistry
IL	Interleukin
iNOS	Inducible nitric oxide synthase
ITAM/ITIM	Immunoreceptor tyrosine-based activation/inhibitory motif
LPS	Lipopolysaccharide
M1	Classically activated macrophage
M2	Alternatively activated macrophage
MCSF	Macrophage colony stimulating factor
mTOR	Mammalian target of rapamycin
NDS	Normal donkey serum
NF-kB	Nuclear factor k B
NK	Natural killer cells
NO	Nitric oxide

PBS	Phosphate buffered saline
PBST	0.3% Triton X-100 in PBS
PCR	Polymerase chain reaction
PDGF	Platelet-derived growth factor
PDK	Phosphoinositide-dependant kinase
PFA	Paraformaldehyde
PH	Pleckstrin homology
PIK	Phosphoinositide kinase domain
PI3-kinase	Phosphatdiylinositiol 3-kinase
PKB	Protein kinase B
PKC	Protein kinase C
PLC	Phospholipase C
PTB	Phosphotyrosine-binding domain
PtdIns	Phosphatidylinositiol
Pten	Phosphatase and tensin homolog deleted on chromosome ten
Rac1	Ras-related C3 botulinum toxin substrate 3
RBD	Ras binding domain
ROI	Region of interest
ROS	Reactive oxygen species
Rtk	Receptor tyrosine kinase
S6K	S6 kinase
SALS	Sporadic form of amyotrophic lateral sclerosis

SH2	Src homology 2 domain
Shc	Src homology 2 domain-containing protein
SHIP	SH2 domain-containing inositol 5’ phosphatase
Sos	Son of sevenless
TGF-B	Transforming growth factor B
Th1	T helper cell type-1
Th2	T helper cell type-2
TNF	Tumour necrosis factor

1: INTRODUCTION

1.1 Amyotrophic lateral sclerosis

Amyotrophic lateral sclerosis (ALS), commonly known as Lou Gehrig's disease, is an adult onset neurodegenerative disease characterized by selective motor neuron loss (Eisen and Krieger, 1998). ALS has a prevalence of approximately 5 per 100,000 people (Julien, 2001) and predominantly affects males (Eisen and Krieger, 1998). ALS is ultimately fatal, and progresses rapidly over the course of 3-to-5 years. The disease is marked by hyperreflexia, muscle atrophy and weakness, speech and/or swallowing difficulties, muscle paralysis and death due to respiratory failure (Julien, 2001; Krieger et al., 1996).

Approximately 5 to 10 % of ALS cases are inherited, or familial, and of all familial ALS (FALS) cases, approximately 20 % have been linked to mutations in the *ALS1* gene that encodes for Cu/Zn superoxide dismutase 1 (SOD1) located on chromosome 21 (Gurney et al., 1994; Rosen et al., 1993). The enzyme SOD1 normally catalyzes the conversion of superoxide radicals to hydrogen peroxide and oxygen (Rosen et al., 1993). The remainder of non-inherited ALS cases are called sporadic (SALS), and are of unknown cause, although the current understanding of ALS is that multiple factors may be involved in the etiology of the disease, including of oxidative stress, excitotoxicity by glutamate, inflammation and an immune-mediated response, as well as the presence of

abnormal intermediate filament accumulations in motor neurons and altered mitochondrial function (Bruijn et al., 2004; Strong and Kesavapany, 2005).

Currently there is no cure for ALS, nor is there any single diagnostic test; however, having a greater understanding of the complex cascade of events which lead to the selective death of motor neurons may lead to these aims. In the current study, an animal model expressing the SOD-1 mutation of ALS was used to further characterize the pathogenesis of motor neuron degeneration and evaluate the possible role of inflammation in the central nervous system (CNS), associated with the innate (non-specific) immune-mediated response (Moisse and Strong, 2006).

1.2 Signal transduction pathways

1.2.1 Phosphatidylionsitol (3,4,5)-triphosphate

Phosphatidylinositol (3,4,5)-triphosphate, commonly abbreviated as PtdIns(3,4,5)P3, is a potent second messenger found on the cytosolic side of eukaryotic cell membranes (Hawkins et al., 2006) that has been identified as a particularly important intermediate of multiple downstream signalling functions such as cell proliferation, differentiation, activation, migration and cell survival (Helgason et al., 1998; Vanhaesbroeck et al., 2001).

As a member of the phosphatidylinositol group, PtdIns(3,4,5)P3 is structurally comprised of a glycerol backbone, 2 hydrophobic fatty acids which are typically stearate and arachidonate, a negatively charged phosphate group and a hexahydric alcohol called inositol (see Fig. 1; Hawkins et al., 2006).

Phosphatidylinositols can be phosphorylated and dephosphorylated at any one or more of the free hydroxyl groups on the inositol ring, with the D-3, D-4, and D-5 positions being phosphorylated on PtdIns(3,4,5)P3. With respect to PtdIns(3,4,5)P3, levels at the plasma membrane are regulated by; 1) the enzymatic class I phosphatidylinositol 3-kinases (PI3-kinase), which phosphorylate the D-3 position of the inositol ring; 2) the ubiquitously expressed, 54 kDa suppressor, Phosphatase and tensin homologue deleted on chromosome 10 (PTEN), which is a phosphatidylinositol 3'-phosphatase that converts PtdIns(3,4,5)P3 to phosphatidylinositol 4,5-bisphosphate [PtdIns(4,5)P2]; and 3) Src homology 2 domain-containing inositol phosphatase (SHIP-1), which converts PtdIns(3,4,5)P(3) to phosphatidylinositol 3,4-bisphosphate [PtdIns(3,4)P2] by the removal of a phosphate group from the D-5 position of the inositol ring (Gloire et al., 2007; Helgason et al., 1998) . The pathways for formation and breakdown of any of these phospholipids is not fully understood. It is thought however, that the formation of Ptdlns(3,4,5)P3 results in the major output signal of activated PI3-kinases (Hawkins et al., 2006).

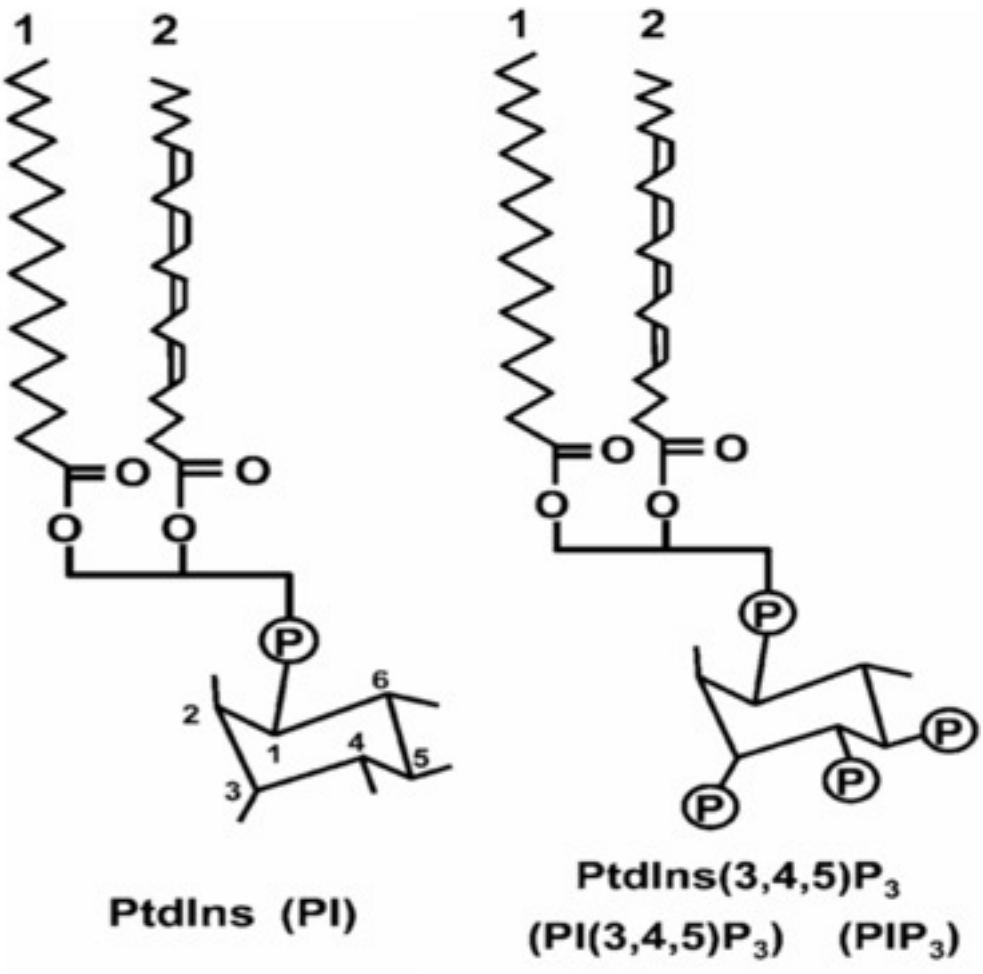

Figure 1 Structure of phosphatidylinositol

Phosphatidylinositols (Ptdlns) are comprised of 2 hydrophobic fatty acids which are esterified to a glycerol backbone, a negatively charged phosphate group and inositol, an hexahydric alcohol group. The inositol can be phosphorylated at the D-3, D4, and D-5 positions to generate different phosphoinositide derivatives with such as PtdIns(3,4)P2 or PtdIns (3,4,5)P3. Reproduced with permission, from Hawkins et al., 2006, Signalling through Class I PI3Ks in mammalian cells, Volume 34, pp. 647-662. © the Biochemical Society.

1.2.2 Phosphatidylinositol 3-kinase

Serving to phosphorylate the 3'-position of the inositol ring of phosphatidylinositols, the signal transduction enzyme phosphatidylinositol 3-kinase (PI3-kinase) generates second messengers such as monophosphates (i.e. PtdIns(3)P), bisphosphates (i.e. PtdIns(3,4)P2), and the trisphosphate PtdIns(3,4,5)P3), all of which act as membrane docking sites for a wide range of downstream effector proteins (Cantley, 2002; Engelman et al., 2006). PI3-kinase activity has been implicated in playing a role in numerous biological processes such as: cell growth, proliferation, survival, differentiation, and cytoskeletal development (Camps et al., 2005; Vanhaesebroeck et al., 2001); furthermore, deregulation of PI3-kinase is thought to play a role in the development of many pathological conditions and the focus of much research has been directed at inhibition of this enzyme with the goal of developing pharmaceutical agents that target allergic responses, inflammation, heart disease, and cancer (Camps et al., 2005; Stein and Waterfield, 2000).

Three conventional classes of the PI3-kinases have been identified (class Ia and Ib, class II, and class III), all of which differ by catalytic and regulatory subunit composition and substrate affinity (Engelman et al., 2006; Hawkins et al., 2006; Vanhaesebroeck et al., 2001). In mammals, it is the class Ia PI3-kinase that primarily mediates the formation of PtdIns(3,4,5)P3 in response to activation by growth factors (Fruman et al., 1998; Wymann and Pirola, 1998). This class has been implicated as a leading regulator of mitogenic signaling (Kapeller and Cantley, 1994). Class Ia PI3-kinases express three catalytic subunits (p110α p110β and p110 δ) and five regulatory subunits (p50α, p55α, p55γ, p85α, and

p85β), which function as adaptor proteins and form heterodimeric complexes that are categorized according to the associated regulatory and catalytic subunits (Engelman et al., 2006; Fruman et al., 1998; Hawkins et al., 2006; Vanhaesebroeck, 1999; Wymann and Pirola, 1998).

The ubiquitously expressed p110 subunit consists of five domains. First is the regulatory or adaptor binding unit (ABD) and a protein binding domain for the guanosine-nucleotide-binding protein ras (RBD), which lies in the N-terminus of p110 and mediates its interaction with Ras-GTP. Next are the PI3-kinase accessory (helical) motif, also known as the phosphoinositide kinase (PIK) domain which is thought to be involved in substrate presentation, and a C2 domain that has been proposed to play a role in membrane association and attachment. The p110 subunit also includes a kinase catalytic domain located at the c-terminus region which contains an ATP-binding site. The catalytic domain permits the binding and subsequent addition of a phosphate group from ATP to the inositol ring of phosphoinositides (Hawkins et al., 2006; Vanhaesebroeck and Waterfield, 1999).

The regulatory subunit of the class Ia PI3-kinase is comprised of an N-terminal SH3 domain, 2 proline-rich regions which flank a break point cluster (BH) domain, also known as a breakcluster region (bcr), and two tandem Src homology 2 or Rous-sarcoma-oncoprotein homology-2 (SH2) domains which are separated by an inter-SH2 region that is responsible for binding to the p110 subunit (Engleman et al., 2006; Wymann and Pirola, 1998). The two SH2 domains are also recognized by a p85 SH2-domain recognition motif on the

inositol phosphatase SHIP-1, and the regulatory domain can bind the full-length tyrosine-phosphorylated SHIP-1 (Engleman et al., 2006).

The main function of p85 is to recruit p110 to tyrosine phosphorylated proteins at the plasma membrane, such that the p110 catalytic subunit is able to phosphorylate available lipid substrates. The BH domain of p85 may also stimulate GTP hydrolysis of small GTP-binding proteins specific to that of the Rho family of GTPases, such as the Ras-related C3 botulinum toxin substrate1 (Rac1) and cell division cycle 42 (Cdc42), both proteins involved in regulating actin structures. Additionally, the SH3 domain located at the N-terminus region of the p85 subunit can bind proline-rich motifs both within p85 itself and in members of the Src family of kinases (Wymann and Pirola, 1998).

Interaction of the p85/p110 complex is mediated by the inter-SH2 domain region of the adaptor-like p85 and the N-terminus of p110. At rest, the regulatory domain constitutively binds and inhibits the p110 unit, although following direct or indirect interaction of the SH2 domains by phosphotyrosine residues, specifically within pYXXM (Y, tyrosine; X, any amino acid; M, Methionine) sequences on tyrosine kinase receptors or receptor-associated adaptor signaling molecules, a conformational change of the regulatory unit relieves the inhibition of the catalytic subunit and mediates its recruitment from the cytoplasm to the inner leaflet of the plasma membrane. Thus, allowing the active heterodimer complex to translocate within close proximity to the phosphoinositide substrate PtdIns(4,5)P2 (Wymann and Pirola, 1998). For example, platelet derived growth factor (PDGF) receptors exhibit intrinsic tyrosine kinase activity and display docking sites composed of

phosphotyrosine residues, and binding at the SH2-domains can activate the p85/p110 signaling complex.

The PI3-kinase complex can also be indirectly activated via the receptor-associated adaptor signaling proteins insulin receptor substrate 1 and 2 (IRS1/IRS2), where the adaptor proteins bridge the interaction of insulin receptors and PI3-kinase SH2 domains PI3-kinase through the interaction of phosphotyrosine residues.

A third method of PI3-kinase activation involves direct binding of the p85/p110 complex to the active or GTP-bound form of the proto-oncogene ras at the RBD on p110. Ras activation is regulated in sequence by guanine exchange proteins (GEPs) and GTPase-activating proteins (Olson and Marais, 2000; Stephens et al., 2000), first requiring recruitment of the adaptor proteins Shc, GRB2 and GAB2 to the plasma membrane following direct association with RTKs, and particularly the Src family of protein tyrosine kinases. The GTP-bound or active form of Ras is then able to associate with GAB2 and bind p110, although with lower affinity than that found between p85 and p110.

1.2.3 Phosphatidylinositol 3-kinase down stream pathways

The membrane recruitment and high-affinity binding of adaptor and effector proteins with PI3-kinase's lipid intermediate, PtdIns(3,4,5)P3, occurs via the recognition of pleckstrin homology (PH) domain-containing proteins, globular protein domains of the N-terminus region that span apknoproximately 100-to-120 amino acids in length. PH domain recognition not only facilitates the translocation of primary target proteins from the cytosol, but also their enzymes and substrates

that are required for catalytic activity (Katso et al., 2001; Vanhaesebroeck and Waterfield, 1999). PH domain-containing proteins recruited to PtdIns(3,4,5)P3 include; 1) guanine nucleotide exchange factors (GEF) such as Vav, which is recruited for the small GTPase, Rac, and relates to actin polymerization and cell motility; 2) tyrosine kinase proteins belonging to the Tec superfamily such as the Bruton's tyrosine kinase (Btk), which is involved in intracellular calcium mobilization; and 3) serine-threonine kinases (Katso et al., 2001) including protein kinase-B (PKB/AKT), a protein that is involved in cell survival, and its activating kinase 3-phosphoinositide-dependent kinase 1 (PDK1) (Paez and Sellers, 2003). The role of PI 3-kinase also encompasses the activation of extracellular signal-regulated kinase (ERK), a member of the mitogen-activated protein kinase family (MAPK) (Vanhaesebroeck and Waterfield, 1999; Toker et al., 1994), through Ras activation, ultimately affecting cell proliferation and cell differentiation through association with cyclinD1, a regulator of cyclin dependant kinases which regulate both entry and progression in the course of the cell cycle. Collectively, these interactions allow the control over downstream cellular processes that ultimately control major biological events within the cell.

1.2.4 Phosphatidylinositol 3-kinase and protein kinase-B signalling pathway

Protein kinase B (PKB) is a key molecule of the PI3-kinase downstream pathway that plays a significant role in the regulation of the cell survival and cell death pathways (Paez and Sellers, 2003). Overall, PKB functions to suppress apoptosis by phosphorylating Bcl-2-associated death promoter (BAD), pro-

caspase 9, and Forkhead transcription factors. The phosphorylation of BAD promotes binding of BAD and the regulatory protein 14-3-3, in turn, inhibiting its association with two anti-apoptotic proteins called Bcl-2 and Bcl-xL (Dudek et al., 1997; Paez and Sellers, 2003). PKB phosphorylation also inhibits activation of the executor caspases (Cardone et al., 1998), and Forkehead, a pro-apoptotic transcription factor that up-regulates the expression level of Fas ligand (FasL). Similar to BAD, when Forkhead is phosphorylated it associates with the 14-3-3 protein and inhibits apoptosis (Brunet et al., 1999; Paez and Sellers, 2003).

PKB phosphorylation also results in downregulation of glycogen synthase kinase 3 (GSK3) activity, and disinhibtion of Cyclin D1; thus, advancing entry and progression through the cell cycle. Additionally, PKB activation of NF-κB, which is essential for inflammation and the innate immune response against bacterial infection, suppresses apoptosis following degradation of an inhibitory protein, IκBα (Paez and Sellers, 2003; Viatour et al., 2005). PKB activation results in phosphorylation of mammalian target of rapamycin (mTOR), which sequentially triggers activation of the S6 kinase (S6K). The S6-kinase plays a crucial role in the progression of cells between the G1 and S phases of the cell cycle and links transcription and translation processes through the phosphorylation of eukaryotic translation initiation factor 4E (eIF4E) binding proteins or 4E-BPs (Dennis and Jaeschke, 2001; Gingras et al., 2001; Paez and Sellers, 2003).

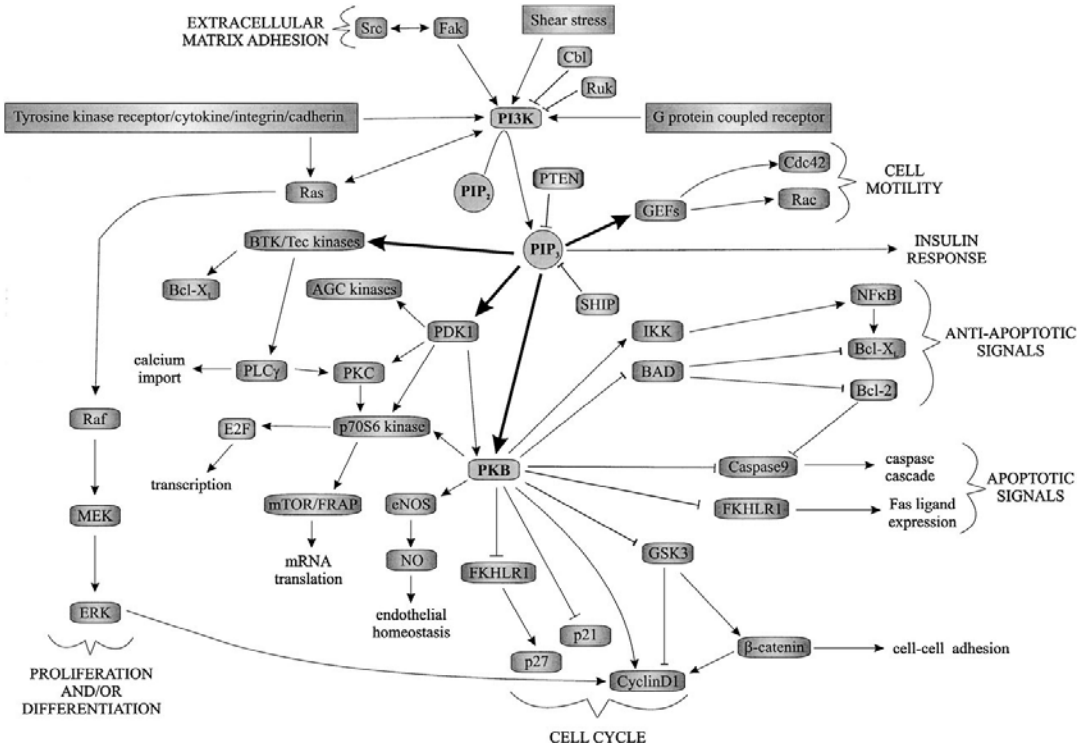

Figure 2 Phosphatidylinositol 3-kinase pathway

Downstream of phosphatidylinositol 3-kinase (PI3-kinase), numerous pathways can be activated, largely through phosphorylation of the PH-domain containing protein PKB. Biological functions including cell motility, cell proliferation and/or differentiation, cell survival and death pathways as well as progression through the cell cycle are regulated through PI3-kinase phosphorylation. Reprinted, with permission, from the Annual Review of Cell and Developmental Biology, Volume 17 © 2001 by Annual Reviews www.annualreviews.org

1.2.5 Phosphatidylinositol 3-kinase and amyotrophic lateral sclerosis

A number of signaling molecules downstream of PI3-kinase and PKB are involved in either promoting cell survival or cell death. Altered protein expression and activity of PI3-kinase and PKB are implicated in the development of pathological conditions such as cancer, characterized by uncontrolled cell proliferation, suppressed apoptosis, and aberrant protein transcription (Vivanco and Sawyers, 2002). Although these processes are incompletely understood, deregulation of these pathways may contribute to the progressive and selective loss of motoneurons noted in ALS.

Under normal circumstances, the PI3-kinase/PKB pathway functions to inhibit apoptosis through regulation of the protein Bad, pro-caspase 9 and transcription factor Forkhead. Surprisingly, analyses of post-mortem tissue from patients who died with ALS compared with control patients have shown that particulate fractions of the spinal cord tissue from patients with sporadic ALS have demonstrated elevated PI3-kinase activity (Wagey et al., 1998), and elevated expression of downstream proteins including PKB and S6K, when compared to control patients (Hu, 2003). Similarly, increased PKB expression has been detected in denervated skeletal muscle tissues of mouse models of human ALS (Cunningham, 2005), and an up-regulation of these PI3-kinase-associated mechanisms may indicate a compensatory mechanism for slowing motoneuron loss, at end-stage of the disease, when neuron loss is most pronounced.

On the other hand, assessment of spinal motoneurons from mouse models of ALS, have shown decreased PI3-kinase and PKB immunoreactivity at the early and pre-symptomatic stages of motoneuron loss (Warita et al., 2001), when compared to wild-type tissue, prior to any significant loss of motoneurons. The reason behind the contrasting results has not yet been elucidated, but may represent differences in the disease stages, which are known to be associated with varying degrees of spinal motor neurons loss, as well as the different tissue samples used for analyses.

1.3 Src homology 2 domain-containing inositol-5' phosphatase

1.3.1 SHIP-1 regulatory domains

Src homology 2 domain-containing inositol 5' phosphatase-1 (SHIP-1) is a 145-kD protein composed of 1190 amino acids in humans (Rohrschneider et al., 2000), with a 96% identity between human and murine SHIP-1 (Ware et al., 1996). SHIP-1 is highly expressed in hemopoietic cells (Krystal et al., 1999; March and Ravichandran, 2002; Pesesse et al., 1997). In addtion to the full-length SHIP-1, there are also cleavage fragments of 135, 125, and 110 kDa derived from the cleavage of the C-terminal proline-rich region (Huber et al., 1999). There is also the closely related family member Src homology 2-containing inositol 5' phosphatase-2 (SHIP-2), which is 1258 amino acids in length with considerable structural and functional identity to SHIP-1 in the catalytic region. In contrast, SHIP-2 is ubiquitously expressed and not restricted to hematopoietic cells (Krystal et al., 1999; Pesess et al., 1997).

SHIP-1 is composed of three distinct regions; 1) an amino-terminal Src homology 2 domain, 2) a central catalytic domain, and 3) a proline rich carboxy-terminus (March and Ravichandran, 2002). The SH2-domain at the N-terminal region of SHIP-1 spans approximately the first 100 amino acids and is capable of binding to tyrosine phosphorylated immunoreceptor tyrosine based inhibition motifs (ITIM) within the cytoplasmic tail of the inhibitory receptor FcyRIIB. FcyRIIBs bind the Fc portion of IgG and negatively regulates B cell receptor (BCR)-dependent B cell activation (Coggeshall, 1998; March and Ravichandran, 2002; Tridandapani et al., 1997a), and through interaction of ITIM-bearing receptors, SHIP-1 negatively regulates cell differentiation and proliferation, as well as other events including PtdIns(3,4,5)P3 induced intracellular Ca^2+ release and extracellular Ca^2+ entry. Similarly, stimulation of SHIP-1 deficient mast cells with B cell produced IgE has been found to result in elevated PtdIns(3,4,5)P3 levels (Huber et al.,1998) and mast cell degranulation, or the rapid release of cytotoxic molecules (Damen et al., 2001; Huber et al., 1998). In addition to ITIMs, the N-terminus can also bind the Ras adaptor protein Shc, where the SH2-domain is thought to compete with and displace the cytosolic adaptors Grb2/Sos complex required for Ras activation (Coggeshall, 1998). Inhibiting Ras activation in turn prevents Ras-induced PI3-kinase activation through binding of the p110 subunit (Chacko et al., 1996; Coggeshall, 1998; Tridandapani et al.,1997b). The SH2 region of SHIP-1 also interacts with other proteins including the ITAMS, Doks, and others (Sly et al., 2004).

The central catalytic 5'-phosphoinositol phosphatase region spans 400-500 amino acids, (Rohrschneider et al., 2000), and is of particular importance as it dephosphorylates the inositol ring at the 5' position (March and Ravichandran, 2002; Sly et al., 2004), producing the lipid product PtdIns(3,4)P2 and downregulates PtdIns(3,4,5)P3-dependant pathways.

The carboxy-terminal of SHIP-1 spans 350 amino acids (Rohrschneider et al., 2000) and is a non-catalytic region of SHIP-1. This region, however, is important for the recruitment of SHIP-1 to the plasma membrane during inhibitory signaling and the stabilization of protein-protein interactions at the plasma membrane (Aman et al., 2000). The carboxy-terminus is composed of a proline rich sequence that constitutively binds the SH3 domain-containing proteins such as the family of activating Src-kinases and the Ras adapter protein Grb2 (Rauh et al., 2003), and ITIM signaling motifs of FcyRIIB (March and Ravichandran, 2002). The c-terminus also displays two NPXY (N, Asparagine; P, proline; X, any amino acid; Y, tyrosine) motifs that provide docking sites for proteins such as Shc, when phosphorylated (Damen et al., 1996; Huber et al., 1999; March and Ravichandran, 2002).

Figure 3 Representation of the domain structure of SHIP-1

SHIP-1 is comprised of an N-terminus src-homology 2 domain that mediates interactions with immunotyrosine motifs and adaptor proteins. At the C-terminus region, two NPXY motifs can bind phosphotyrosine binding domain containing proteins and proline rich sequences can bind Src homology 3-containing proteins. The catalytic domain is centered between two regions of unknown function, and regulates the inositol phosphatase activity of SHIP-1. Modified with permission from Rohrschneider et al., 2000, Structure, Function, and Biology of the Ship Proteins, Volume 14, pp. 505-520. © Genes and Development.

1.3.2 Expression and distribution of SHIP-1

The SHIP-1 protein is expressed in cells of the hematopoietic lineage (Krystal et al., 1999; Liu et al., 1998; March and Ravichandran, 2002) such as granulocytes, lymphocytes, monocytes and progenitors (Liu et al., 1999), with differential expression of various SHIP isoforms having been detected in cells of the bone marrow and blood (Geier et al., 1997). SHIP-1 protein expression also appears to vary during the process of hemopoiesis, and increases substantially during T cell maturation (Liu et al., 1998) and during activation of resting B cells (Brauweiler et al. 2001).

The notion that SHIP-1 is restricted to hematopoietic cells, as early as at the onset of hematopoesis, is widely accepted based on studies investigating the expression of SHIP-1 in various tissues and cell types. Interestingly, Northern blot analyses of mRNA isolated from mouse embryos indicate that SHIP-1 is actually expressed in the primitive stage of embryo development at approximately 7.5 to 8.5 days postcoitus, and is expressed in embryos that differentiate into both hematopoietic cells and endothelial cells (Liu et al., 1998). However, hematopoietic stem cells and endothelial cells originate as the same mesenchymal primitive cell, the embryonic hemangioblast, and SHIP-1 is not expressed in endothelial cells once differentiated into distinct cell populations (Liu et al., 1998). Furthermore, recent investigations into the expression of phosphoinositide phosphatase in relation to insulin regulation have claimed that there is no significant immunoreactivity against SHIP-1 in the hypothalamic arcuate and lateral nuclei (Bertelli et al., 2006).

The inositol phosphatase SHIP-2, shares several structural and functional properties with SHIP-1; however, SHIP-2 is ubiquitously expressed and not restricted to hematopoietic cells, as indicated by the prominent levels of expression found in muscle and nervous (i.e. neurons, astrocytes and oligodendrocytes) tissues (Muraille et al., 2001). In tissue, SHIP-1 is expressed in the testis, lung and liver (Liu et al., 1998), with notably high expression in the spleen (Helgason et al., 1998). Increased SHIP-1 expression in the spleen, a lymphoid organ, coincides with the occurrence of extramedullary haematopoiesis that has been observed in SHIP-1 deficient mice (Helgason et al., 1998).

1.3.3 Mechanism of action of SHIP-1

The negative regulatory action of SHIP-1, to reduce the levels of PtdIns(3,4,5)P3, is exerted in a sequential manner and is conditional upon two primary factors; 1) prior phosphorylation of the 3'position of the inositol phospholipid PtdIns(4,5)P2; and 2) recruitment of SHIP-1 from the cytosol to the plasma membrane (Krystal et al., 1999; Rohrschneider et al., 2000).

SHIP-1 has been shown to be phosphorylated by the family of Src-kinases, however, phosphorylation of SHIP-1 is not sufficient to alter the catalytic activity of SHIP-1. The mechanism of action for SHIP-1 first requires initial receptor activation, and after receptor stimulation (i.e. cytokine receptor or immunoreceptor), SHIP-1 is then recruited to the plasma membrane (Sly et al., 2003) by the SH3-domain of the c-terminus region, and can then bind the phosphorylated tyrosine residues on activated receptors with one or both SH-2 domains located within the N-terminus region.

The collective recruitment, binding and activation of SHIP-1 promotes the hydrolysis of PtdIns(3,4,5)P3 by association with its centrally located phosphoinositol phosphatase domain. Overall, this activity results in negative regulation of downstream signal transduction pathways via protein-protein interactions that are intiated by domain recognition and the binding of specific phosphotyrosine residues, as identified in the previous section.

1.3.4 SHIP-1 and the inhibition of PKB downstream pathways

The role SHIP-1 plays in negatively regulating biological functions such as cellular growth and survival, through the regulation of PI3-kinase, can be evaluated using SHIP-1 deficient mice. SHIP-1 deficient mice exhibit constitutive PKB activation and increased expression of PtdIns(3,4,5)P3 (Horn et al., 2004; Liu et al., 1999), both effects indicating the role SHIP-1 plays in regulating PI3-kinase downstream targets by dephosphorylating PtdIns(3,4,5)P3, the lipid product of PI3-kinase activity.

Irregular myeloproliferation occurs in SHIP-1 deficient mice (Helgason et al., 1998). As such, SHIP-1 may have powerful tumor suppressor-like function (Liu et al., 1999; Luo et al., 2003), supporting a role for SHIP-1 in the negative regulation of PI3-kinase/PKB signaling in hematopoeitic cells (Aman et al., 1998). PI3-kinase/PKB signaling has been found to play an important role in the development of human tumors and has become a promising target for cancer therapy (Horn et al., 2004; Luo et al., 2003). For example, at a cellular level the role of SHIP-1 has been analyzed in the human leukemia Jurkat line, a T-cell line established from a patient with acute lymphoblastic leukemia, whereby the

endogenous expression of SHIP-1 is lost and PI3-kinase and PKB are constitutively activated (Luo et al., 2003). Similar to findings at the tissue and systemic levels in mice, as a result of a SHIP-1 deficiency in Jurkat cells, an irregular rate of cellular growth and proliferation have been observed and are thought to be attributed to the hyperphosphorylation of PKB downstream targets such as GSK3, a major constituent involved in the regulation of the cell cycle process (Horn et al., 2004).

The involvement of SHIP-1 in cell cycle regulation and survival is also apparent through the evaluation of other PKB downstream targets such as NF-κB. Activation of NF-κB is a hallmark of inflammation, and is induced by exposure to pro-inflammatory cytokines such as TNF-α. When activated, NF-κB enhances cell proliferation and anti-apoptotic gene expression, and also promotes angiogenesis via expression of endothelial growth factors. Altered NF-κB activation is caused by deregulated and often constitutive phosphorylation of NF-κB, and has been found to be a major contributor to chronic inflammatory diseases (Viatour et al., 2005). On the other hand, SHIP-1 has been shown to dampen the response to pro-inflammatory mediators, at least in part by reducing NF-KB-dependent transcription activity (Liu et al., 1999b).

Overall, the role that SHIP-1 plays in the regulation of events downstream to PI3-kinase activity is crucial for maintaining controlled cellular growth, proliferation, and survival. Research investigating the characteristics of animal models deficient in SHIP-1 has demonstrated the importance of PI3k-kinase downregulation and the contribution of SHIP-1 to controlling pathways

downstream of PI3-kinase, which are regulated by the phosphorylation of PKB. The manner in which SHIP-1 dampens the response to pro-inflammatory mediators will be further discussed in the subsequent section, with specific emphasis on inflammation and the involvement of SHIP-1.

1.4 The innate immune system

1.4.1 Macrophage development and activation

Macrophages, or in the CNS, microglia, are highly responsive to their environment, and are characterized by a marked phenotypic heterogeneity which is dependent upon the presence or absence of particular environmental stimuli. Through early observations first noted by Stein et al., (1992) a model of two major macrophage classes was developed which mirror the T helper cell type 1 (Th1) and T helper cell type 2 (Th2) nomenclature that is characteristic of the pro-inflammatory and anti-inflammatory responses of T cells respectively. As such, "alternatively" activated macrophages, or M2 cells have a functional phenotype distinct from what are now called "classically" activated macrophages, or M1 cells (Mantovani et al., 2007). Both the M1 and M2 phenotypes are important constituents of the immune response; notably, the M1 macrophage subtype promotes inflammation and tissue injury, whereas the M2 macrophage subtype tends to resolve inflammation and facilitate wound healing (Mantovani et al., 2007).

The M1 macrophage resembles the Th1-like phenotype by acting as an effector cell or pathogen killing cell through the promotion of inflammation, extracellular matrix (ECM) destruction, and apoptosis. M1 macrophages rapidly

respond to a large variety of acute pathological stimuli in the form of microbial agents and T helper cell type 1 (Th1) cytokines, including the transcription factor tumor necrosis factor-α (TNF-α), macrophage colony-stimulating factor (M-CSF), a stimulator of hematopoeitic cell differentiation, or interferon-γ (IFN- γ), and exhibit significantly high levels of IL-12, a potent stimulator of TNF and IFN-y production, and IL-23 which is critical for the generation of the T cells that produce other pro-inflammatory proteins, and low levels of the anti-inflammatory cytokine IL-10, a down-regulator of Th1 cytokine expression (Mantovani et al., 2007). The M1 macrophage phenotype is also marked by inducible nitric oxide synthases (iNOS) expression, whereby iNOS metabolizes L-arginine to generate the large amounts of nitric oxide (NO^-), and also releases pro-inflammatory cytokines such as IL-1β, TNF-α, and IL-6.

The M2 macrophage subtype acts to dampen the pro-inflammatory response, scavenge debris, and promote tissue remodeling and repair, and angiogenesis. M2 macrophages are commonly associated with chronic infections and allergic responses, and after exposure to the appropriate stimuli such as the Th2 cytokines IL-4, IL-13 or IL-10, secrete high levels of IL-1 and IL-10 and release TGF-ß for ECM building and reconstruction. M2 macrophages also upregulate the enzyme arginase I which is involved in the biosynthesis of proline for ECM construction and tissue repair, as well as polyamines which promote cell proliferation. Other factors secreted by the M2 macrophage include platelet-derived growth factor (PDGF), which is known for its significant role in angiogenesis, insulin-like growth factors (IGF), one of the most potent natural

activators of the PKB signaling pathway, and transforming growth factor beta (TGF-ß) which is involved in the regulation of cell growth, cell differentiation, and survival.

1.4.2 Microglial cells

Microglia are resident immunocompetent cells of the nervous system and are the equivalent of tissue-specific macrophage populations (van Rossum and Hanisch, 2004; Vilhardt, 2005), constituting between 10 and 20 % of the non-neuronal cells in brain parenchyma. Not to be confused with the macroglia, microglia differ in origin from that of ectoderm derived astrocytes and oligodendrocytes, and arise from the hematogenous monocyte/macrophage lineage from mesoderm (Barron, 1995; Sargsyan, Monk and Shaw, 2005).

For many years, glia were believed to be simple supportive structural elements of the nervous system despite the fact that they out number neurons at least ten to one in the human brain (Kandel, 2000); however, even in what has been defined as “resting” or “quiescent” state, it is now known that their highly ramified morphology exhibit processes that allow for continuous immune surveillance of the CNS parenchyma (Nimmerjahn et al., 2005; van Rossum and Hanisch, 2004) and cross-talk with other glial cells and neurons (Vilhardt, 2005). Furthermore, in an activated state microglia retract their processes, shifting morphologies whilst concomitantly exerting functions that parallel all tissue-resident macrophages including phagocytosis, induction of inflammation, and antigen presentation (Aloisi, 2001).

In recent years, microglia involvement in the first line of immune defence in the CNS has been studied considerably, while directing efforts towards understanding their function in an inflammatory state. What is known is that in an immune response, microglia have the potential to undergo dramatic morphological and functional changes from a "resting" ramified form, to an "active" amoeboid form typical of the macrophage-like morphology (Kreutzberg, 1996; Sedgwick and Hickey, 1997). However, functional aspects of the microglia responses as they relate to various pathologies, including neurodegenerative disease, are not fully understood.

1.4.3 The role of microglia in ALS

A dramatic increase in activated microglia cell expression has been widely detected in pathologically affected areas of both post-mortem tissues of human ALS patients, and in mouse models of the disease suggesting that microglia are involved in ALS (Hall et al., 1998; Kawamata et al., 1992). However, it is not clear whether microglia have neuroprotective or neurodegenerative effects.

Microglia are heterogeneously distributed throughout the brain and spinal cord, are most prominent in grey matter regions and in close proximity to neurons, and to a lesser extent between fiber tracts in white matter (Stoll et al., 2002). Corresponding to the motor involvement of ALS, evaluation of spinal cord tissue of murine models of human ALS, have shown a significant increase in number of activated microglia located in the vicinity of degenerating motor neurons, and such changes have been recognized as a feature of ALS disease progression (Wootz, 2006). In the current study, the spinal cord from mouse a

model of ALS was evaluated to assess the inflammatory state of microglia cells. The degree of co-localization with SHIP-1, a down-regulator of the pro-inflammatory response, was assessed as a means of determining the phenotypic nature of the microglia.

1.5 SHIP-1 function and the innate immune response

1.5.1 The SHIP-1 knockout mouse model

The functional role of SHIP-1, has been clarified through the creation of the SHIP-1 knockout mouse model that was developed by deleting the first exon of the SHIP gene located on chromosome 1C5 (Helgason et al., 1998) (2q36/37 in humans; Sly et al., 2007). The SHIP-1 deletion is specific to SHIP-1 and has no effect on the expression of the alternate splice form SHIP-2 (Helgason et al., 1998).

SHIP-1 is an endogenous inhibitor of the PI3-kinase pathway, when faced with the appropriate stimuli, SHIP-1 becomes phosphorylated and suppresses the activation of the PI3-kinase and downstream pathways. Presumably resulting from chronically elevated PtdIns(3,4,5)P3 levels (Rauh et al., 2005) and at least in part, sustained phosphorylation of PKB, SHIP-1 deficient mice have been found to be overly sensitive to cytokines and growth factors, and overproduce granulocyte-macrophage progenitors in both bone marrow and spleen (Helgason et al., 1998; Kim et al., 1999) due to a lack of control over cell growth, proliferation and survival/death pathways. Furthermore, SHIP-1 knockouts exhibit severe pulmonary inflammation and fibrosis, and a significantly shortened lifespan due to the infiltration of highly proliferative neutrophils, macrophages,

and natural killer (NK) cells which display an increasing number of inhibitory receptors (Helgason et al., 1998).

With respect to the immune response, SHIP-1 has also been found to play a role in determining macrophage phenotype, as SHIP-1 deficient mice express constitutively high levels of arginase-1, and therefore diminished levels of nitric oxide (NO), as well as significantly lower levels of pro-inflammatory mediators.

1.5.2 SHIP-1 and negative regulation of the pro-inflammatory response

SHIP-1 has been shown to be a prominent regulator of intracellular signalling events involved in maintaining immune homeostasis, and, when required, plays a crucial role in eliciting the appropriate immune response. The role of SHIP-1 in mediating the innate immune response can be best be characterized in macrophages and monocytes, due to the discrete and contrasting patterns of myeloid activation and myeloproliferation that are observed in SHIP-1 expressing and SHIP-1 knockout models (Helgason et al., 1998; Rauh et al., 2005).

In macrophages, SHIP-1 functions to repress the M2 macrophage phenotype, the class of macrophages that play a significant role in rapid tissue remodelling and repair, and serves to down regulate functions such as tumour growth and angiogenesis seen in cancerous tissues (Luo et al., 2003; Rauh et al., 2005). Likewise, in line with the suppression of M2 macrophage activation, SHIP-1 expressing macrophages have a tendency to polarize towards the classically activated phenotype, whilst keeping the pro-inflammatory cycle in-check by negatively regulating PI3-kinase-dependent pathways, such as NFκB-

driven cytokine secretion, and other pathways which are largely regulated by PtdIns(3,4,5)P3 hydrolysis (Rauh et al., 2005).

The role of SHIP-1 in the immune system and inflammation has been well characterized through observations made through the lipopolysaccharide (LPS)-induced macrophage inflammatory response. Exposure to low levels of LPS, which is a potent initiator of the innate immune response secondary to bacterial infection, results in the production of pro-inflammatory cytokines from macrophages and as much as a 10-fold increase in SHIP-1 protein expression (Rauh et al., 2005). Upon subsequent exposure to high levels of LPS, SHIP-1 is thought to play a vital role by reducing further pro-inflammatory cytokine expression via its inhibitory role over PI3-kinase and therefore NFκB activation; thus, playing a protective role to avoid damage resulting from activated immune cells (Liu et al., 1999b). Characteristic of the M2 phenotype, SHIP-1 deficient macrophages on the other hand do not display endotoxin tolerance. SHIP-1 deficient macrophages *in vivo* have been shown to be unable to produce cytokines and inflammatory mediators for fighting infection because of the high level of arginase I (ArgI) that results from increased PtdInds (3,4,5)P3 expression (Rauh et al., 2005; Sly et al., 2004)

Overall, SHIP-1 expressing cells tend to suppress the alternative activation, or anti-inflammatory role, of a macrophage cells in order to combat non-specific immune responses. Additionally, with the activation of SHIP-1 and the production of pro-inflammatory molecules, SHIP-1 protein levels may be substantially up-regulated as a compensatory mechanism in response to the

activation of PI3-kinase downstream signal transduction pathways and associated PtdIns(3,4,5)P3 expression, thereby preventing an aberrant and damaging response.

1.6 Mutant SOD-1 model of ALS

1.6.1 Mutant superoxide dismutase-1 (mSOD-1)

Transgenic mice that over-express a mutant form of human SOD-1 have been used extensively as a mouse model of ALS. Mutations in SOD-1 are found in approximately 2% of all ALS cases, and transgenic mice expressing human mutant SOD-1 are frequently used as they have similarities in pathology and progression to that observed in patients with ALS.

The normal function of the copper/zinc superoxide dismutase (SOD-1) enzyme is to catalyze the conversion of superoxide radicals into hydrogen peroxide (McCord and Fridovich, 1969; Brunori and Rotilio, 1984). There are several hypotheses concerning the role of mutant SOD-1 in ALS, and while the initial belief was that a loss-of-function, or impaired scavenging/antioxidant activity of the enzyme was responsible for the toxic effect of the mutant enzyme (Yim et al., 1996), it is now thought that SOD-1 mutations result in a toxic gain-of-function effect (Gurney et al., 1994). The toxic gain of function has been proposed to be a consequence of the aberrant production of free radicals that are generated in response to elevated production of hydrogen peroxide, a substrate of the dismutatase activity (McCord and Fridovich, 1969; Wiedau-Pazos et al., 1996). The gain of function hypothesis is supported by data showing that mice that do not express SOD-1, following gene knockout, do not develop histological

abnormalities, nor do they develop motor neuron disease or clinical characteristics of ALS, such as muscle atrophy and muscle weakness (Reaume et al., 1996).

1.6.2 G93A mSOD-1 model of ALS

One transgenic mouse model that over expresses a mutant form of the human SOD-1 gene was developed through the substitution of glycine for alanine at position 93 (SOD1 [G93A]). The G93A mutation has been identified as one of the most prevalent of more than 100 identified mutations in SOD-1 in FALS patients, and in mice, over-expression of this mutant results in progressive motoneuron disease (Gurney et al., 1994).

In the G93A mouse model, observable signs typically appear between 80 and 90 days of age and are initially characterized by hind limb tremor and weakness. This is followed by slower than normal rates of growth and muscle atrophy predominating in the hindlimbs which progresses to partial and full hind limb paralysis as a result of motoneuron degeneration at the end-stage of the disease (Chiu et al., 1995; Guegan and Przedborski, 2003). Due to the fact that the phenotype and genotype of the transgenic G93A mSOD-1 model are distinctive of the motor neuron disease ALS, the G93A transgenic mouse is commonly used to investigate the pathology of human ALS and will be used in this study.

2: JUSTIFICATION OF STUDY AND HYPOTHESES

2.1 Justification of study

The overall aim of this thesis was to study the expression of SHIP-1 in the mSOD-1 mouse to gain further insight into the neuropathological characteristics of this murine model of ALS, and determine the potential role of the SHIP-1 protein in the neuropathology. SHIP-1 acts as a negative regulator in many cell-signalling pathways of the immune system and is expressed in hematopoietic cells. To the best of our knowledge, the distribution of SHIP-1 expression has not been previously evaluated using immunohistochemical analyses in microglia. Microglia have the potential to damage neighbouring cells such as motoneurons during prolonged inflammation through the production of inflammatory molecules, and may play a role in the pathogenesis of ALS. As SHIP-1 is a regulator of monocytic function, I explored whether changes in SHIP-1 expression may be implicated in a murine model of motor neuron disease.

2.2 Objectives and hypotheses

Objective 1

To determine whether SHIP-1 is expressed in spinal cord tissue, and whether there are any differences in SHIP-1 expression between mSOD-1 mice and age-matched wild-type controls, using immunohistochemical analysis.

Hypothesis 1

SHIP-1 is up-regulated and translocated to the plasma membrane of haematopoietic cells, to hydolyze PtdIns(3,4,5)P3, during the pro-inflammatory response. In the current study, I hypothesized that SHIP-1 immunoreactivity will increase in the grey matter regions of the mSOD-1 spinal cord tissue, particularly in areas affected by motoneuron loss, such as the ventral horn.

Objective 2

To examine whether SHIP-1 immunoreactivity can be detected in microglial cells using double labelling immunohistochemistry techniques.

Hypothesis 2

Previous research indicates the expression of SHIP-1 is restricted to haematopoietic cells, such as monocytes and macrophages. Prolonged inflammation is associated with ALS, and produces selective motoneuron degeneration and progressive microgliosis, and I hypothesized that SHIP-1 immunoreactivity will be detected in activated microglia, due to the cell lineage and role of SHIP-1 in dampening the inflammatory response.

3: METHODS

3.1 Animals

Transgenic mice from the C57BL6-TgN and B6SJL-TgN strains of SOD1-G93A [(SOD1-G93A)1Gur] and wild-type control mice were used for this study. Mice were bred at the Animal Care Facility (Simon Fraser University) from progenitor stock animals. The transgenic mice have a missense mutation (G93A), over-expressing a mutant form of the human Cu/Zn superoxide dismutase (SOD1) gene (mSOD-1), which contains a glycine to alanine substitution (amino acid 93). This strain of mouse is used as a model of ALS as mice exhibit progressive motor deficits similar to those observed in ALS patients (Gurney et al., 1994).

Symptom onset for the mSOD-1 mouse begins between 80 and 90 days of age, and is characterized by hind limb tremor in the early stage and a progression to progressive fore and hind limb paralysis. To monitor clinical progression, staff at the Animal Care Facility visually inspected mice daily when observable signs were present.

At approximately 16-18 weeks of age, the mice reached end-stage, a time at which mice exhibit very substantial motor deficits. End-stage disease is defined by an inability to recover to a prone position following having been placed on their sides. End-stage mice were sacrificed with a CO2/O2 mixture, and at a time point of approximately 45 s when breathing ceased, but prior to cardiac

arrest, the mice were perfused transcardially with 30 ml of 1x phosphate buffered saline (PBS, 4% w/v, pH 7.4) followed by 30 ml of 4% paraformaldehyde (PFA, 4% w/v, pH 7.4). The spinal cord was then carefully dissected and fixed in 4% PFA before being cryoprotected in 20% sucrose (sucrose 20% w/v in 1X PBS), at 4 C˚ for 24 h. The use of mouse tissue was in accordance with the guidelines set by the SFU Animal Care Committee and the Canadian Council for Animal Care.

3.1.1 Animal genotyping

3.1.1.1 DNA extraction

To identify transgenic progeny, at approximately 1 mo of age, small ear tissue punches were taken from each mouse for genotyping (protocol adapted from Hu et al., 2003). Tissue samples were placed in an autoclaved 1.5 ml eppendorf tube with a 5% Chelex (5% w/v; Fluka) solution in low TE (0.1X Tris-EDTA Butter; pH 7.6) to prepare the DNA template for the polymerase chain reaction (PCR) protocol. The Chelex solution for one sample consisted of Chelex (125ul per sample; Fluka, product ID #95577), Proteinase K (12.5ul per sample; 20mg/ml in ddH20; Sigma-Aldrich, product ID # P-2308) and RNase A (12.5 ul per sample; 10mg/ml in Rnase buffer; Sigma-Aldrich, product ID # R-4876).

The sample and solution combined were placed in a 55°C water bath for 15 min, vortexed for 10 sec and then placed back in the water bath for an additional 15 min. Tubes were incubated in a boiling water bath (100°C) for 8 min and centrifuged for 5 min at 1200 rpm at 4°C to complete DNA extraction. The

supernatant from each sample was transferred into an autoclaved eppendorf tube and used immediately as a DNA template or stored indefinitely at -20°C.

3.1.1.2 Polymerase chain reaction

Polymerase Chain Reaction (PCR) protocols were used to differentiate genotypically “affected” mice from control mice, via use of the mouse genomic DNA extracted for use as a template. Samples were prepared in 25 ul volumes as follows: 1.0 ul of DNA template; 0.5 ul MgCl2; 2.5 ul of 10x buffer and dNTP stock solution (100mM stock); 17.2 ul of distilled H2O; 0.3ul of Taq polymerase (Qiagen product ID # 201205). Primers used include 0.5 ul mSOD1- CAT CAG CCC TAA TCC ATC TGA (forward) and 0.5 ul mSOD2- CGC GAC TAA CAA TCA AAG TGA (reverse), both obtained from Invitrogen. To amplify the DNA, PCR was conducted on the reaction mixture with a thermocycler (Techine TC-3000) using the following temperature cycles: 1 denaturation cycle for 5 min at 95°C, followed by 30 cycles for 30 seconds each at 94°C for denaturation, annealing at 56°C, and extension at 72°C, 1 cycle for 30 sec at 94°C and 56°C, and then a final phase of extension at 10 min at 72°C. The solution was then cooled down to 4°C and stored indefinitely.

3.1.1.3 Sodium dodecyl sulfate polyacrylamide gel electrophoresis

The PCR product was determined by running 1% agarose gel electrophoresis (2 g Agarose, 200 ml 0.5X Tris-Acetate EDTA, 20ul Ethidium Bromide). Samples consisted of 10ul of the PCR product mixed with 2ul of loading dye, and were carefully loaded onto gel lanes (Mupid-21 Mini Gel

Migration Trough, Cosmo Bio Co. Ltd). The gel was covered with a solution of 0.5X Tris-Acetate-butter (1L TAE buffer solution, 242g Tris Base, 57.1ml Acetic Acid, 100ml 0.5M EDTA, 600.9ml ddH20, pH 8.5) and run at a constant voltage of 100V for 45 min. Once finished gels were placed under UV light (Fotodyne, Bio/Can scientific) and photographed. The absence (wild-type) or existence (affected/mSOD-1) of a band of fluorescence at 236 base pairs confirmed the genotype of each animal.

3.2 Immunohistochemistry

3.2.1 Cryosectioning

The spinal cord was cut into three regions at the lumbar, thoracic and cervical levels. Each region was then mounted with optimal cutting temperature medium (Tissue Tek) and sectioned traversely at 30 um, using a Reichert-Jung Cryocut 1800 (Leica) and Feather microtome blades (Tissue Tek). Every 5^{th} section was collected and stored in de Olomos solution in an autoclaved 1.5ml eppendorf tube. Tissue sections were stored indefinitely at -20°C. The cryostat block temperature was set at -17°C.

3.2.2 Immunofluorescence

Sections post-fixed in 4% paraformaldehyde (pH 7.4) were permeabilized with 0.3% Triton X-100 in PBS (0.3% PBST) at room temperature (RT) and subject to antigen-retrieval by incubating the tissue section in a glycine solution (0.5M glycine, 1 h, RT). Non-specific conjugate binding to the SHIP-1 primary

antibody was blocked (1 h, RT) in blocking buffer containing 25 % normal donkey serum (NDS) and 3% bovine serum albumin (BSA).

Spinal cord tissue was incubated overnight at 4˚C, in primary SHIP-1 antibody (optimal dilution of 1:1000) with staining buffer (0.3% Triton X-100, 3% BSA and 10% NDS). Dilutions of 1:200-1:5000 where attempted for all SHIP-1 antibodies to find the optimal concentration.

Tissue sections were rinsed with agitation, in 0.3% PBST the following day. The spinal cord tissue was incubated in staining buffer with cyanine-3 (Cy3, dilution of 1:1000) conjugated anti-IgG for 2 h at RT, and kept in darkness for the remainder of the experiment. Sections labelled with only the secondary antibody served as negative controls.

After agitated rinsing in 0.3% PBST, the spinal cord tissue was incubated in blocking buffer (10% NDS, 3% BSA, 0.3% PBST) for 1 h at RT before double labelling at 4˚C overnight, with one of two antibodies directed against microglia, primary monoclonal rat IgG to Iba-1 (dilution of 1: 1000) or CD11b (dilution of 1:500), also known as macrophage-1 antigen. In other experiments, spinal cord tissue was labelled with rat IgG against anti-glial fibrillary acidic protein (GFPA), an antibody directed against astrocyte intermediate filaments.

Approximately 24 hr following incubation in primary antibody, sections were rinsed in 0.3% PBST, and spinal cord tissue was incubated in secondary antibody such as Alexa647-conjugated donkey anti-rat anti-IgG (dilution of 1:1000) or fluorescein isothiocyanate (FITC, dilution of 1:1000) for 2 h at RT. Sections were washed in 0.3% PBST, slide mounted and air-dried before

applying Vectashield mounting medium (Vector Laboratories Inc.) and applying the cover-slips which were sealed with clear nail polish. Slides were stored in darkness at -20°C for image analysis.

3.2.2.1 Antibodies

Two primary polyclonal rabbit anti-SHIP-1 antibodies were used in the experiments; one SHIP-1 (N-1) antibody was obtained from Santa Cruz Biotechnology (Santa Cruz, CA, USA; product ID # sc-6244), while the other was from StemCell Technologies (Vancouver, BC, Can; product ID # 01506). The antibody from StemCell Technologies was generated against a GST fusion protein corresponding to residues 7-133 of mouse SHIP-1. This antibody targets the SH2-domain of the N-terminal region, and has been reported to be specific for mouse full length SHIP-1 protein (145 kDa) as well as C-terminal truncated forms (135, 125, 110 kDa forms; Damen et al., 1998), whereas the antibody from Santa Cruz Biotechnology was directed against amino acids 1-105 of mouse SHIP-1, at the N-terminal region (recommended optimum of 1:50-1:500). The primary SHIP-1 (P1C1) antibody and the primary SHIP-1 (M-14) antibody were also used in the initial experiments. The SHIP-1 (P1C1) monoclonal mouse anti-SHIP-1 antibody (Santa Cruz, CA, USA; product ID # sc-8425) is directed against amino acids 866-1020, mapping the C-terminal region (recommended optimum of 1:50-1:500) and the SHIP-1 (M-14) polyclonal goat anti-SHIP-1 antibody (Santa Cruz, CA: USA; product ID # sc-1964 is directed against a peptide mapping the C-terminal region (recommended optimum of 1:50-1:500).

Polyclonal rat anti-Iba-1 antibody of mouse origin, directed against the C-terminus region of Iba-1 (dilution of 1:1000, Wako Chemicals, Richmond, VA, USA, Product ID # 019-19741), was chosen to visualize microglia because it is not cross-reactive with neurons and astrocytes. A second marker for microglia, mouse anti-rat CD11b (dilution of 1:500, Serotec, Raleigh, USA; product ID # MCA275A488) was also utilized. The CD11b antibody, also known as Mac-1, is directed against the receptor for the iC3b component of complement, an antigen that is found on most macrophages, including microglia. Monoclonal rat anti-GFAP, (dilution of 1:200; EMD Biosciences, Calbiochem, San Diego, CA, USA; product ID # #345860) was also used to identify astrocytes.

Secondary antibodies included donkey-anti-rabbit-conjugated to cyanine 3 (Cy3, dilution of 1:1500, Jackson ImmunoResearch Labs, West Grove, PA, USA), as well as donkey-anti-rabbit or anti-rat (dependent upon which animal the primary was raised in) Alexafluor647-conjugated anti-IgG (Alexafluor647, dilution of 1:1000; Molecular Probes, Eugene, OR, USA) or anti-rat FITC (dilution of 1:1000; Molecular Probes, Eugene, OR, USA) were used to visualize microglia, astrocytes and SHIP-1 respectively.

3.2.2.2 Image analysis and quantification

Positive SHIP-1 cells and microglia marked by positive Iba-1 staining were analyzed by epifluorescence microscopy (Leica DM4000B). Leica filter cube Texas Red Brightline Filter set was used for Cy3-labelling (emission peak at 570 nm) of SHIP-1 and Leica filter cube Y5 Brightline Filter set was used for Alexa647 staining (emission peak at 670 nm) of Iba-1 or GFAP. The Leica filter

cube L4 FITC Brightline Filter set was used for FITC staining (emission peak at 495 nm). Images were acquired with a Leica DFC 350FX camera and Leica Application Suite software at 4x, 10x, 20x, and 40x magnifications.

To evaluate the SHIP-1 immunoreactivity, lumbar spinal cord sections (n=3) at each time point (11 weeks, 15 weeks and end-stage) were evaluated from the mSOD-1 and age-matched wild-type mice. Three lumbar sections were also evaluated from the SHIP-1 knockout mouse. To quantify immunoreactivity to SHIP-1, cells were visualized through the immunoflurorescence of the secondary antibody Cy3, and then counted manually under low and medium power (10-20x) in the defined anatomical region of interest (ROI). It is recognized that an observer blind to the experimental conditions could have also been used to perform the manual counting and should be employed in future experiments. In the case of multiple observers inter-rater reliability would need to be evaluated. The ROI was defined by a superimposed 90° angle extending from the central canal through the median fissure, and laterally across the grey and white matter regions to the most peripheral point of each section. In order for a cell to be identified as being positive for SHIP-1 immunoreactivity, distinct labelling of SHIP-1 at the plasma membrane had to be present, and the entire cell body had to be localized to the ROI.

Mean differences between the number of SHIP-1 immunoreactive cells that were counted in the mSOD-1 lumbar spinal cords, at 15 weeks and at end-stage, were compared using independent-t tests. Independent-t tests were also used to compare the mean differences in the number of SHIP-1 immunoreactive

cells that localized to the defined ROI's in the ventral and dorsal horns. An $\propto$– level of 0.05 was set as significant for all tests, and all results are reported as means ± SE. All analyses were conducted using the SPSS 17 statistical software.

Images captured were cropped and sized for display purposes before being converted from tiff to jpeg image formats in the Adobe Photoshop 6.0 software program.

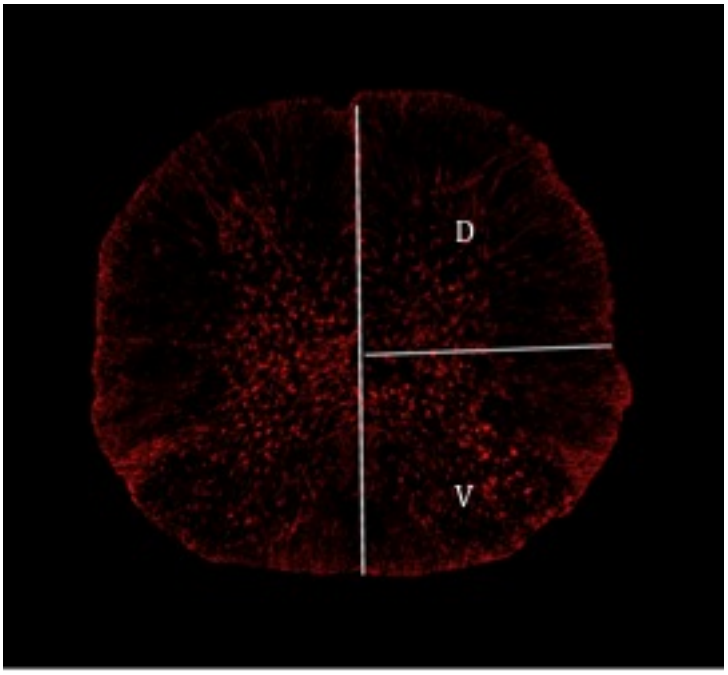

Figure 4 Image analysis and SHIP-1 immunoreactivity quantification

A region of interest (ROI) was defined by the superimposing of a 90° angle extending from the central canal through the median fissure, and laterally across the grey and white matter regions to the most peripheral point of each section. Dividing the section into 2 quartiles allowed for the comparison of the ventral and dorsal regions respectively (v, ventral; d, dorsal). The number of SHIP-1 immunoreactive cells in the ventral and dorsal regions were counted in 3 lumbar spinal cord sections of mSOD-1 and age-matched wild-type mice.

4: RESULTS

4.1 SHIP-1 immunoreactivity

To define the distribution of SHIP-1 immunoreactivity in spinal cord, spinal cord tissue was taken from transgenic G93A mSOD-1 and age-matched wild-type mice, sectioned transversely at a thickness of 30um and examined using immunofluorescence techniques. SHIP-1 immunoreactivity was assessed regionally in the spinal cord including the ventral and dorsal horns, and across three time points in age-matched mSOD-1 and wild-type mice; 11 weeks when mSOD-1 mice are asymptomatic, 15 weeks when mSOD-1 mice exhibit disease symptoms, and at end-stage. SHIP-1 immunoreactivity was determined primarily using antibodies directed against the N-terminal region of the SHIP-1 protein (StemCell Technologies).

As shown in Fig. 5, spinal cord tissue from end-stage mSOD-1 mice exhibited considerable SHIP-1 immunofluorescence, particularly in the ventral horn region of the spinal cord (Fig. 5a). SHIP-1 immunofluorescence exhibited several distinct patterns depending on the region examined. Within the grey matter, immunoreactivity appeared to localize to cellular elements in that immunoreactivity was discrete and not uniform. In contrast, filament-like immunoreactivity was detected in the white matter that ran perpendicular to the surface of the spinal cord in a radial fashion. Within grey matter, SHIP-1 immunoreactivity was more prominent in ventral regions, compared to the dorsal

horns (Fig. 5a and b). The discrete immunoreactivity found in the grey matter is shown under higher power in Fig. 5c.

To further evaluate the regional differences in SHIP-1 expression between the ventral horn and dorsal horn regions in mSOD-1 tissue, the number of SHIP-1 immunoreactive cells, located in the grey matter, were visually counted under the microscope at 20x power. SHIP-1 immunofluorescence was compared between the right ventral horn and right dorsal horn quadrants in end-stage mice, according to defined regions of interest (Fig. 4) and an independent t-test (2-tailed) was carried out. The regional difference in the number of SHIP-1 immunoreactive cells that were counted manually in the ventral horn (M=113.3 ± 4.9, n=3) and dorsal horn (M=103 ± 5.1, n=3) regions of 3 lumbar sections, was not statistically significant in the end-stage mSOD-1 spinal cord [$t(2)=1.4$, $p>0.05$].

In contrast to the end-stage mSOD-1 mice, age-matched wild-type mice at all 3 time points, and SHIP-1 knockout mice, exhibited no discernable SHIP-1 labelling. Furthermore, when comparing SHIP-1 expression in tissue of 11-week-old asymptomatic mSOD-1 mice to tissue of SHIP-1 knockout mice or wild-type mice at any time point, there was also no difference in SHIP-1 expression (Fig. 6 and Fig 7).

Assessment of 15-week-old mSOD-1 tissue revealed distinct cellular staining that predominantly localized to the ventral horn region of the spinal cord. Unlike the end-stage mice, the regional difference in the mean number of SHIP-1 expressing cells counted in the ventral horn (86.7 ± 2.3 cells, n = 3) and dorsal

horn (63.3 ± 3.2 cells, n=3) regions was statistically different [$t(2) = 5.9$, $p < 0.05$]. When compared to end-stage mSOD-1 mice, a 1.4 fold increase in the mean number of SHIP-1 expressing cells that were counted in both the dorsal and ventral horn regions combined, was noted between the 15 week (150.0 cells ± 5.5, n=3) and end-stage (216.3 ± 3.9 cells, n=3) time points (Table. 1). Furthermore, the percentage of SHIP-1 expressing cells counted in the ventral horn region of the spinal cord, when compared to the total number of SHIP-1 expressing cells counted in both the ventral and dorsal spinal cord regions, was lower in the end-stage spinal cord when compared to 15 week spinal cord tissue. SHIP-1 immunoreactivity had a tendency to become more evenly distributed in the grey matter at end-stage. A total of 57.8% of the total number of SHIP-1 immunofluorescent cells localized to the ventral horn region in the spinal cord at 15 weeks (ventral= 86.7 ± 2.3 vs dorsal= 63.3 ± 3.2, n=3), whereas 52.2% of the total number of SHIP-1 immunofluorescent cells counted at end-stage (ventral=113.3 ± 4.9 vs dorsal= 103.0 ± 5.1, n=3) localized to the ventral horn region (Table 2; Fig. 8).

A second antibody targeting the N-terminal region of SHIP-1 (N-1, SantaCruz Biotechnologies) as well as two antibodies targeting the C-terminal region of SHIP-1 (P1C1 and M-14, SantaCruz Biotechnologies) were used to assess tissue from end-stage mSOD-1 and age-matched wild-type controls; however, no specific SHIP-1 immunoreactivity was identified using this antibody (data not shown). I do not have a good explanation as to why I did not obtain clear labelling with these antibodies.

Number of SHIP-1 expressing cells	11 week old n=3	15 week old n=3	end-stage n=3
mSOD-1	0	150 ± 5.5	216.3 ± 3.9
wild-type	0	0	0

Table 1 Immunoreactivity of SHIP-1 in the spinal cord of mSOD-1 mice and age-matched wild-type mice.

Immunoreactivity was evaluated at 11 week, 15 week and end-stage time points by mannually counting the number of SHIP-1 immunoreactive cells in the lumbar spinal cord (n=3). Number of cells expressed as mean ± SEM.

Regional distribution of SHIP-1 cells	Ventral horn n=3	Dorsal horn n=3	Total count n=3
15 week mSOD-1	86.7 ± 2.3	63.3 ± 3.2	150 ± 5.5
end-stage mSDO-1	113.3 ± 4.9	103.3 ± 5.1	216.3 ± 3.9

Table 2 Regional distribution of SHIP-1 immunoreactivity in the lumbar spinal cord of mSOD-1 mice at 15 weeks and end-stage timepoints.

The number of SHIP-1 immunoreactive cells counted in the ventral horn regions and dorsal horn regions of the lumbar spinal cord (n=3) were statistically different ($p < 0.05$) at the 15 week timepoint but not at disease end-stage. A tendency for SHIP-1 immunoreactivity to be more evenly distributed throughout the gray matter of the spinal cord was noted. Number of cells expressed as mean ± SEM.

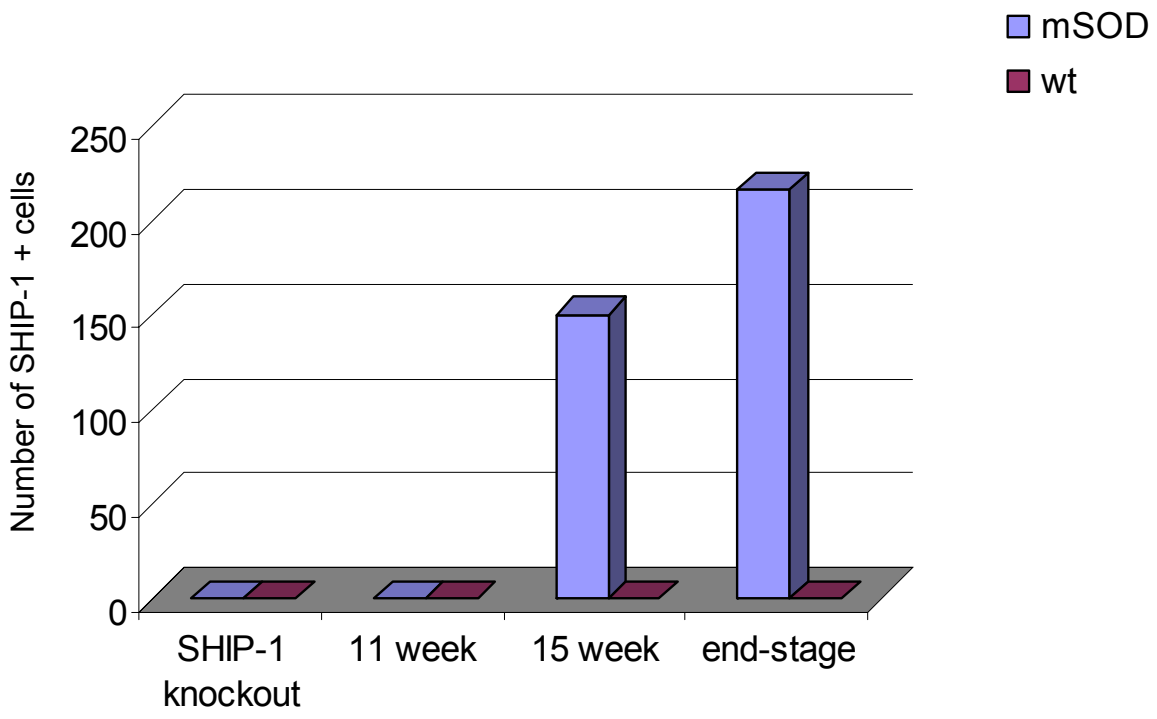

Figure 5 SHIP-1 expression in mSOD-1, wt and SHIP-1 knockout mice

Immunoreactivity of SHIP-1 was compared across three time points in the mSOD-1 mice; 11 weeks when mSOD-1 mice are asymptomatic, 15 weeks when mSOD-1 mice exhibit disease symptoms, and at end-stage. The number of SHIP-1 positive cells counted in the ROI, increased in the mSOD-1 tissue at symptom onset (M=150) and was greatest and end-stage (M=216). No SHIP-1 expression was found in 11 week old mSOD-1 tissue, wild-type mice at any time point, or SHIP-1 knockout mice.

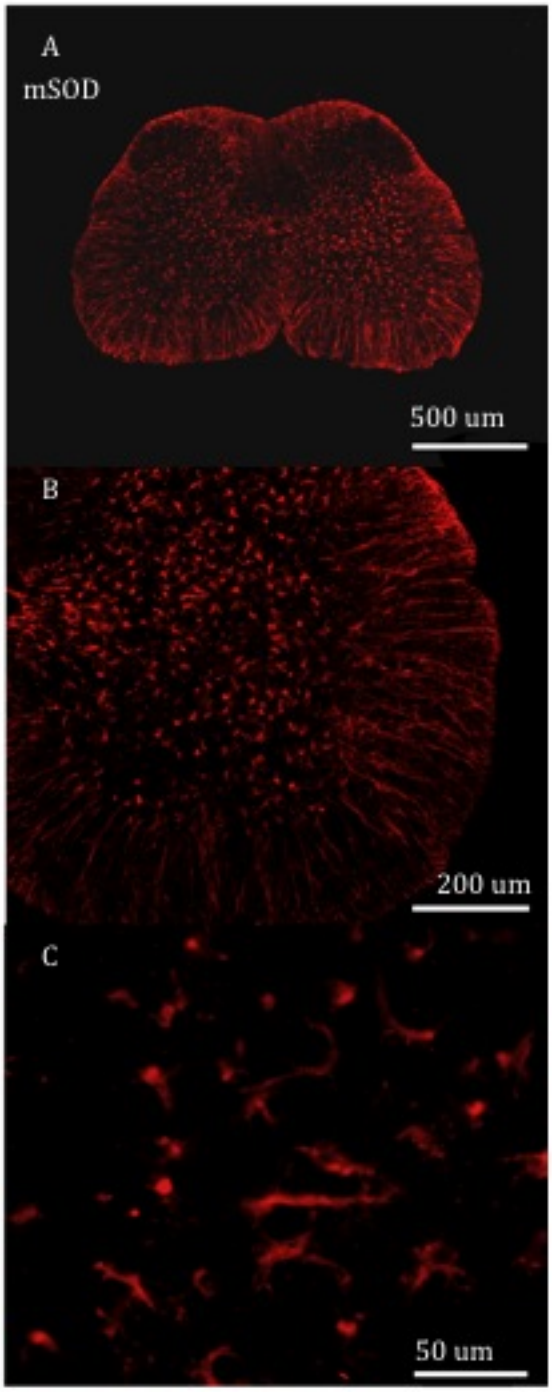

Figure 6 Immunoreactivity of SHIP-1 in the spinal cord of end-stage mSOD-1 mouse

Red channel shows SHIP-1 immunoreactivity visualized with Cyanine-3 at 4x (a), 10x (b) and 20x (c) magnifications. Scale bars represent 500 um, 200 um, and 50 um.

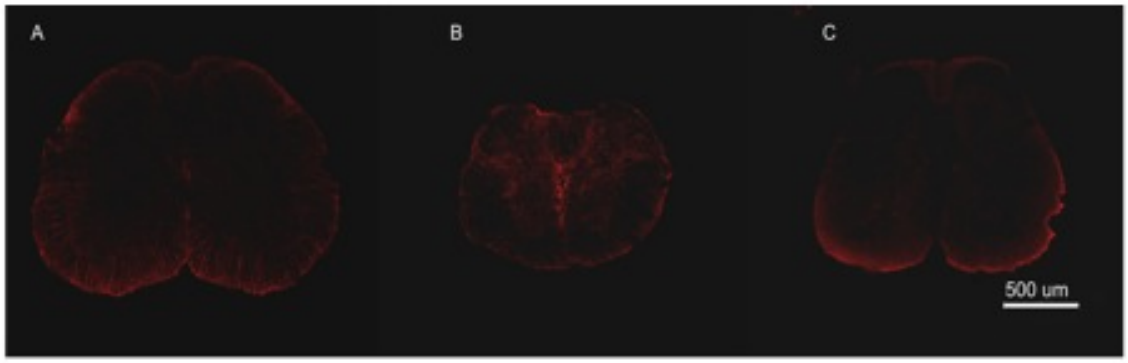

Figure 7 Comparison of SHIP-1 immunoreactivity in control tissues

SHIP-1 immunoreactivity in transverse section of spinal cord in wt mice (a), SHIP $^{-/-}$ mice (b) and age-matched control tissue lacking the primary SHIP-1 antibody (c). Immunohistochemistry failed to detect any discernable SHIP-1 labelling in wt mice, SHIP-1$^{-/-}$ mice and tissue lacking the primary SHIP-1 antibody. Scale bar represents 500 um.

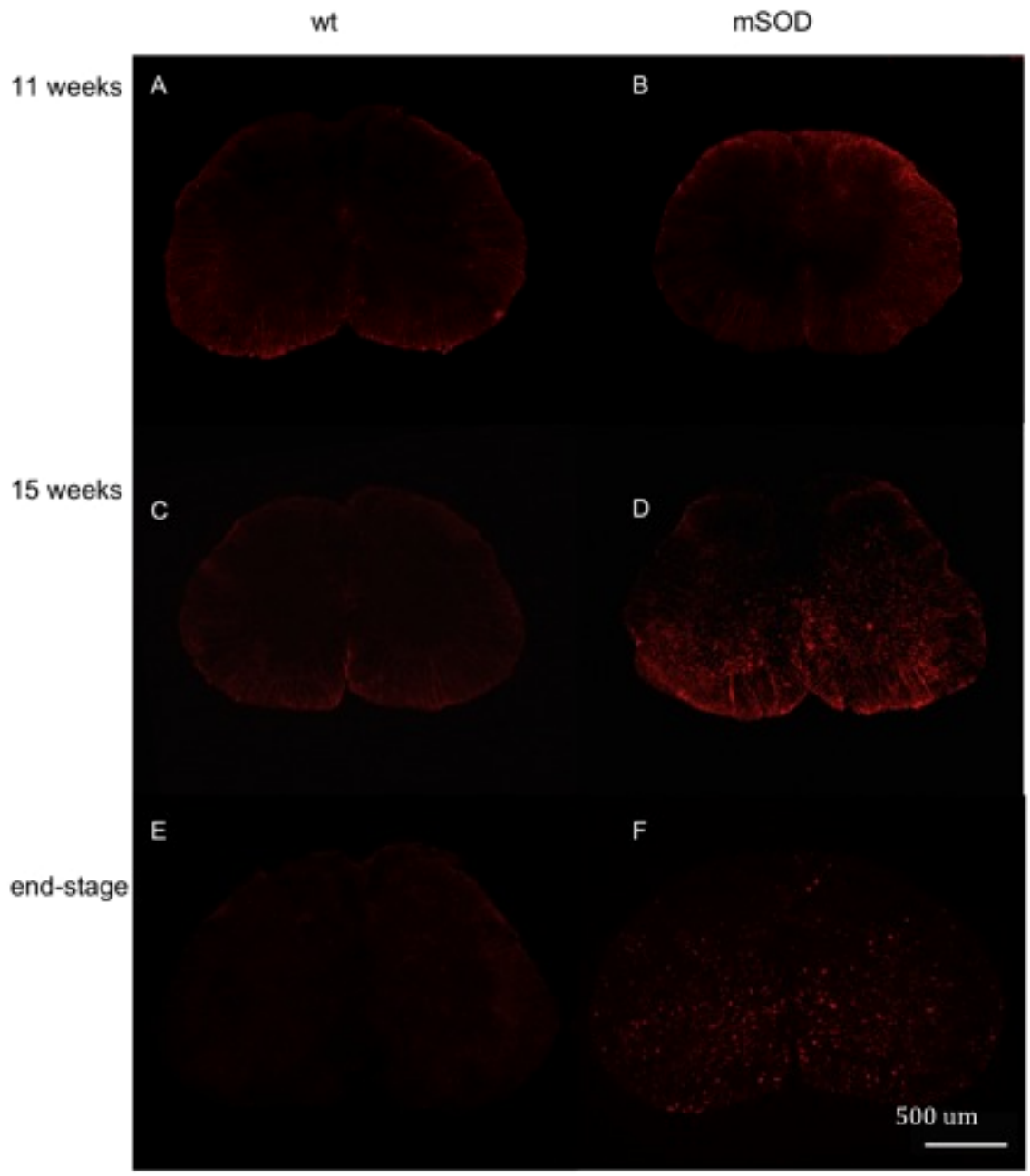

Figure 8 Transverse sections of spinal cord from mSOD-1 and wt mice

Disease progression is illustrated at 3 time points, asymptomatic (11 weeks), symptomatic (15 weeks) and end-stage, and analyzed by immunofluorescence techniques. Using antibodies directed against SHIP-1, an increase in SHIP-1 expression in spinal cord sections of mSOD-1 mice was detected, when compared to age-match controls, at 15 weeks and end-stage time points. No difference in SHIP-1 expression was observed between the 11 weeks mSOD-1 and wt groups at either 15 weeks or end-stage time points. Scale bar measures 500 um in length.

4.2 Morphological phenotype of SHIP-1 immunoreactive cells

Within the grey matter of spinal cord morphological features of SHIP-1 expressing cells were variable. Many of the cells observed were star or stellate-shaped and had small cell bodies and long, narrow, spiny or radial-like processes. Other cells appeared larger in overall size, and exhibited more rounded cell bodies with thicker but shorter processes. Immunolabelling was largely cytoplasmic and membrane-associated with extension into processes. In most cells, there was no evidence of nuclear labelling (Fig 9B). Morphological differences, particularly with respect to cell body size, appeared to coincide with changes in SHIP-1 expression, or SHIP-1 staining intensity (Fig. 9).

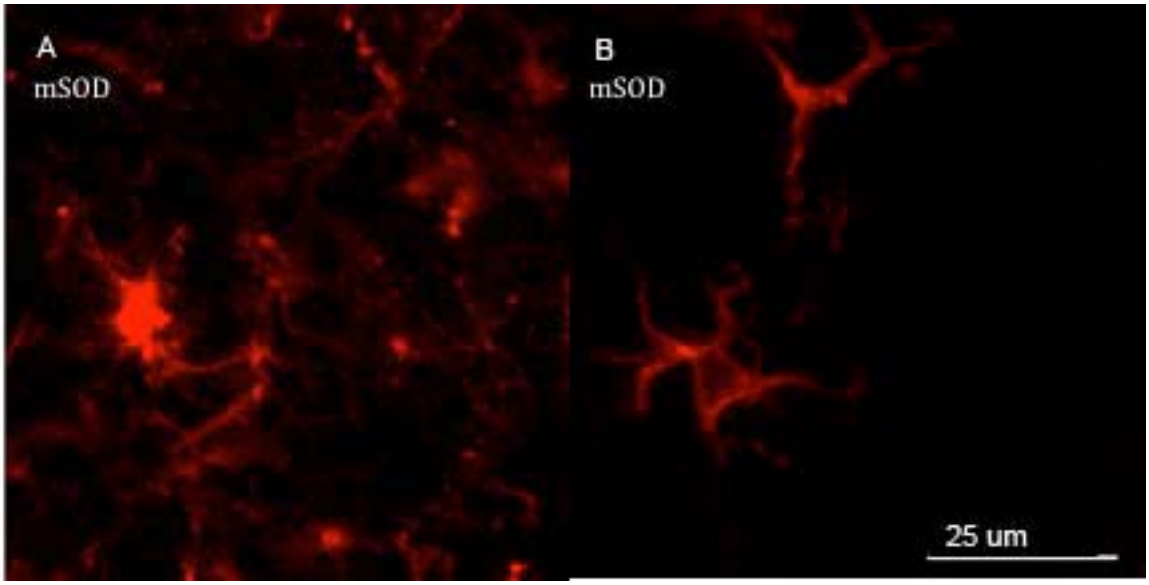

Figure 9 Morphological phenotype of SHIP-1 immunoreactive cells

Transverse sections of spinal cord of mSOD-1 mice at end-stage. SHIP-1 expressing cells varied in morphological phenotype, ranging from large and ameboid shaped cell bodies with thick short processes (a), to long, thin or narrow shape cells having small rod-like shaped cell bodies (b).

4.3 SHIP-1 co-localization in glia cells

Profuse microglia and astrocyte proliferation and activation have been shown to correlate with increased production of inflammatory molecules in the G93A mSOD-1 model of ALS (Hall et al., 1998), as well as in post-mortem tissue of human ALS patients. Additionally, with respect to previous research, the number of microglia (Iba1+ and CD11b+ cells) and astrocyte (GFAP+) cells visualized with immunofluorescence has been found to increase substantially, when compared to age-matched wild-type mice.

In the current study, antibody directed against GFAP was used to assess astrocyte activation and recruitment, and anti-Iba1, anti-CD11B antibodies were used to detect microglia/macrophage activation and recruitment. Immunohistochemistry using cell-specific markers was performed to identify localization patterns of SHIP-1 expression in specific cell types, and to determine whether SHIP-1 was expressed in cells of the hematopoietic lineage, including microglia/macrophage cells. Interestingly, antibodies against SHIP-1 and epitopes of microglia/macrophage cells did not reveal co-localization of SHIP-1 and microglial/macrophage in 15 week old or end-stage mSOD-1 tissues where SHIP-1 expression was noted (Fig. 10 and Fig. 11). The increased GFAP expression visualized in 15 week old and end-stage mSOD-1 tissues co-localized extensively with SHIP-1, suggesting SHIP-1 expression was limited to astrocytes (Fig. 12).

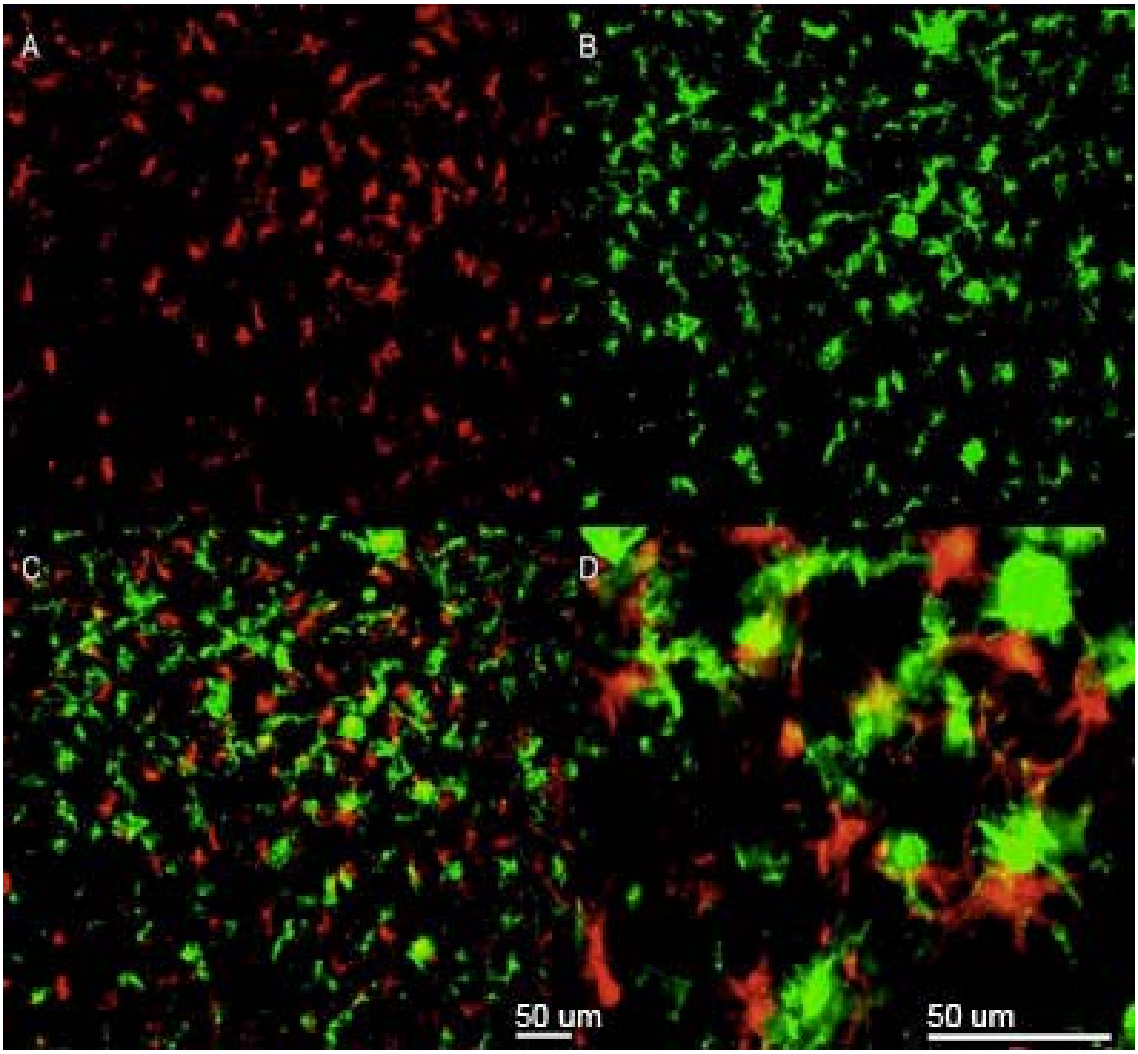

Figure 10 Double labelling with SHIP-1 and Iba-1 marker for microglia

Immunohistochemistry of spinal cord section of mSOD-1 mice. Red channel shows SHIP-1 expression (a); green channel shows microglia cell marker Iba-1 (b); no discernable double labelling is illustrated in SHIP-1 and Iba-1 merged images (c,d). Scale bar represents 50 um at low (10x) and high (40x) power magnifications.

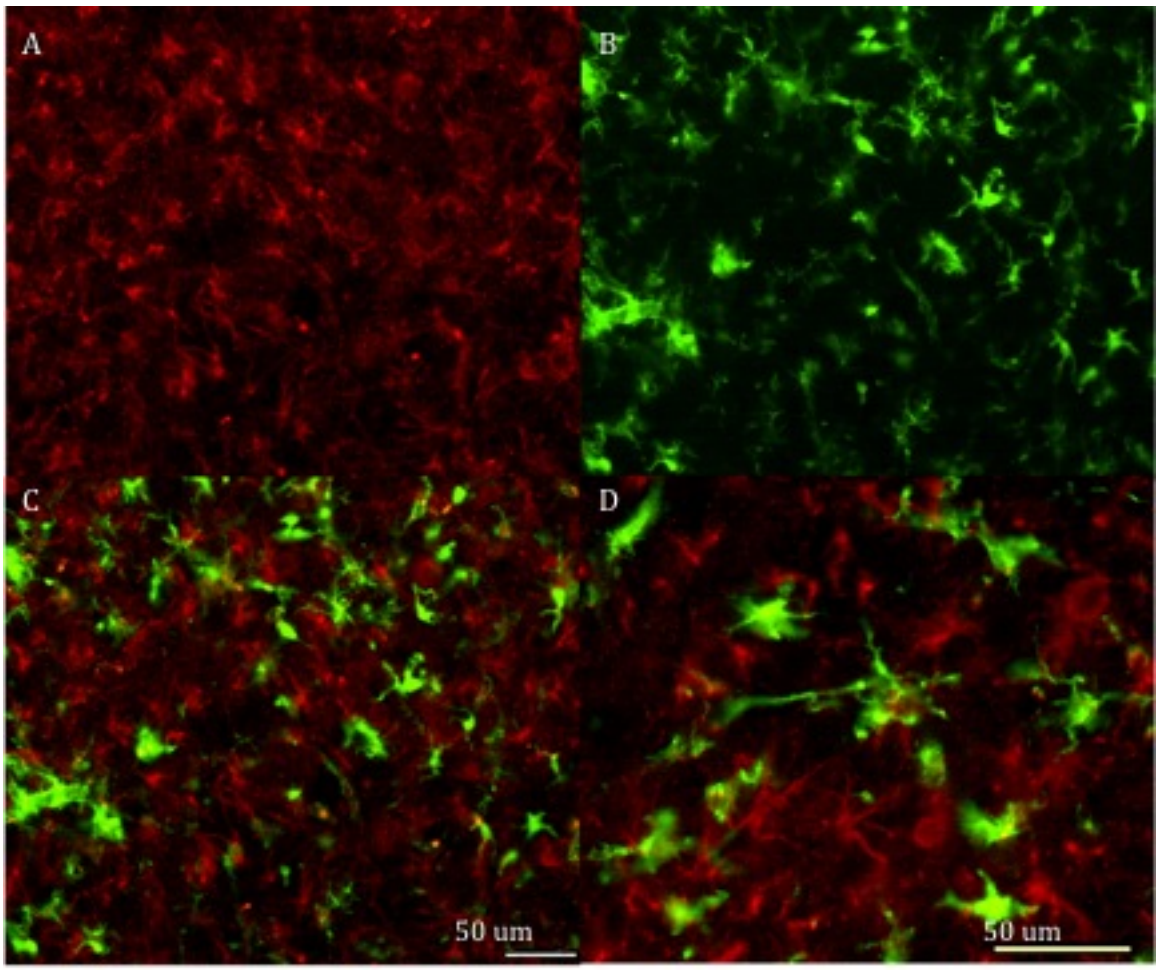

Figure 11 Double labelling with SHIP-1 and CD11b marker for microglia

Immunohistochemistry of spinal cord section of mSOD-1 mice. Red channel shows SHIP-1 expression (a); green channel shows microglial cell marker CD11b (b); no discernable double labeling is illustrated in SHIP-1 and CD11b merged images (c,d). Scale bar represents 50 um at low (20x) and high (40x) power magnifications.

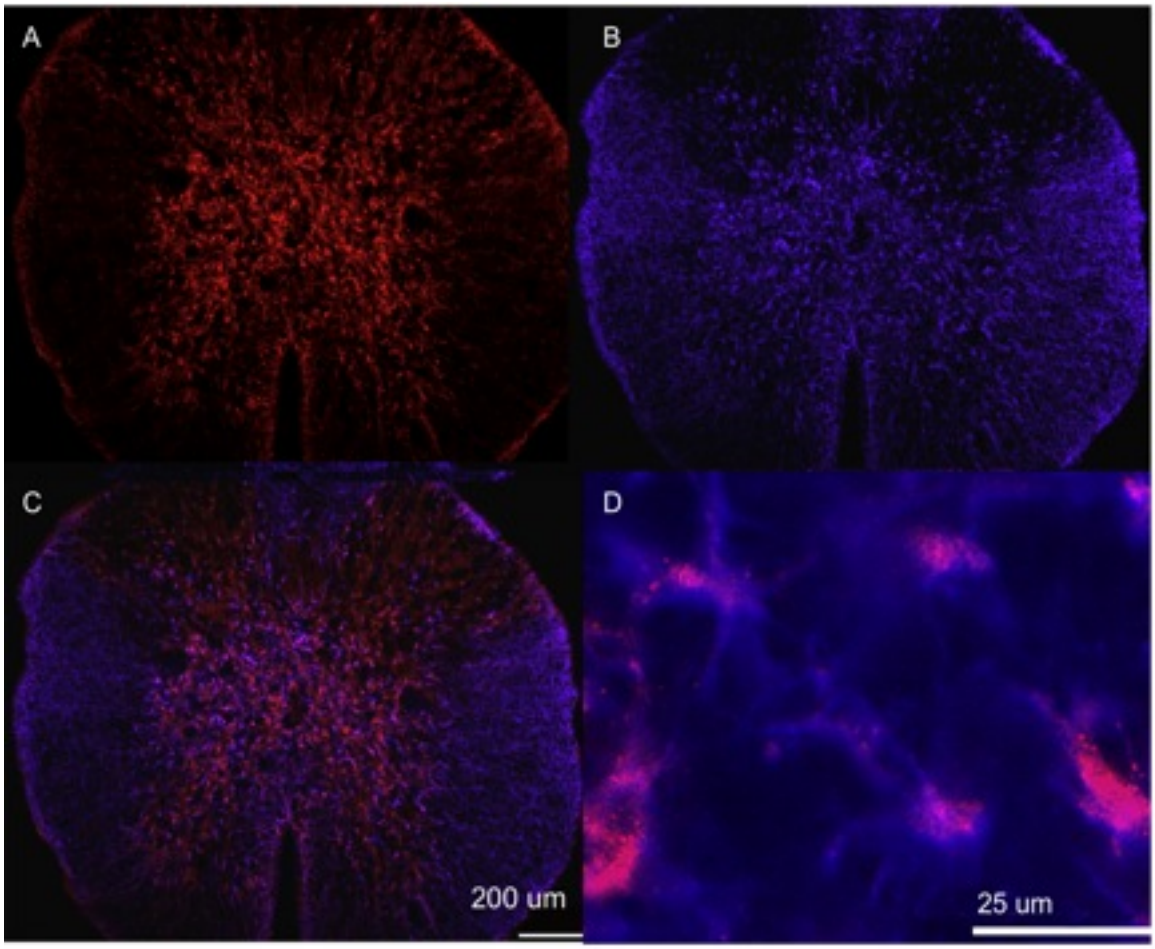

Figure 12 Double labelling with SHIP-1 and GFAP marker for astrocytes

Immunohistochemistry of spinal cord section of mSOD-1 mice. Red channel shows SHIP1 expression (a); green channel shows astrocyte cell marker GFAP (b); merged image shows double labelling of SHIP-1 positive and GFAP positive cells (c,d). Scale bar represents 200 um at low (10x) and 25um at high (40x) power magnifications

5: DISCUSSION

Even though ALS is not recognized as a classic immunological disorder, current data suggest that inflammation is a marker of disease progression (Wootz, 2006) such that inflammatory mediators can be detected in the CNS, prior to any development of phenotypical manifestations of the disease (Alexianu et al., 2001). With respect to ALS, inflammation itself is also believed to contribute to the damage and loss of motoneurons and recent studies have shown that mSOD-1 microglia induce more motoneuron death when compared to wild-type SOD-1 expressing microglia, due in part to increased production of nitric oxide and superoxide, and reduced production of growth factors (Xiao et al., 2007). There are multiple aspects of neuroinflammation, however, and the capacity for inflammatory mediators to favour tissue damage in one instance and protective mechanisms in another (Wootz, 2006), makes it difficult to assess the significance and reasoning for inflammation in the pathological state.

In the current study, SHIP-1, which is known to play a key role in regulating the inflammatory response through its course of action of hydrolyzing PtdIns(3,4,5)P3 (Gloire et al., 2007; Helgason et al., 1998), was studied to further characterize the inflammatory state of mSOD-1 microglia. More specifically, the goal of this study was to characterize the distribution of SHIP-1 in spinal cord, and to determine if SHIP-1 immunoreactivity was altered in the G93A mSOD-1 mouse model of ALS.

5.1 Elevated SHIP-1 immunoreactivity in the spinal cord of mSOD-1 mice

To evaluate SHIP-1 immunoreactivity I employed a commercial rabbit polyclonal antibody generated against a GST fusion protein corresponding to residues 7-133 of mouse SHIP-1. This antibody targets the SH2-domain of the N-terminal region. The antibody has been reported to be specific for mouse full length SHIP-1 protein (145 kDa) as well as C-terminal truncated forms (135, 125, 110 kDa forms; Damen et al., 1998). Immunoreactivity against SHIP-1 was observed in spinal cord from mSOD-1 mice. This immunolabelling likely represents specific labelling of SHIP-1 protein as: 1) it was confined to specific cell types in a cytoplasmic distribution, 2) it was not observed when the primary antibody was omitted, and 3) this labelling was not observed in tissue obtained from SHIP-1 knockout mice. I attempted to obtain further validation that the antibody was specific for SHIP-1 by two other commercial antibodies obtained from a different biotechnology company, including a mouse monoclonal anti-SHIP-1 antibody that was directed against amino acids 866-1020 of the C-terminus of SHIP-1 (antibody P1C1), and a rabbit polyclonal antibody (N-1) that was directed against amino acids 1-105 of the N-terminus region. In experiments using both the M-14 and P1C1 antibodies, labelling in spinal cord tissue was inconsistent and punctate, and did not correspond to an intracellular distribution. Although these antibodies have been reported to be useful for immunofluoresence, there is little literature supporting the distribution of immunoreactivity in specific cell types, and no literature to support the successful use of either antibody in CNS tissue. Furthermore, it is possible that the

inconsistency of labelling with P1C1 could be due to the use of a mouse monoclonal antibody to label mouse tissue. As a result of the variability in these observations, the data shown in the thesis are derived from original experiments using the polyclonal rabbit anti-SHIP-1 antibody exclusively. I attempted to perform internal controls by labelling spleen tissue using this polyclonal anti-SHIP-1 antibody, as hematopoietic cells have been previously reported to express SHIP-1 (Helgason et al., 1998); however, immunolabelling of the spleen tissue was poor for reasons which were unclear.

Experiments using the polyclonal anti-SHIP-1 antibody demonstrated immunolabelling within the grey matter of spinal cord in mSOD-1 mice and no specific cytoplasmic labelling in age-matched wild-type mice. To substantiate a relation between SHIP immunoreactivity and disease progression in mSOD-1 mice, I labelled spinal cords from mSOD-1 mice at various ages, and SHIP-1 immunolabelling was not detected in asymptomatic mSOD-1 mice, but was detected in symptomatic mice at 15 weeks of age and at end-stage, a time at which mice were exhibiting very substantial motor deficits. SHIP-1 immunoreactivity was observed to be greatest at the end-stage time point, as determined by both the overall intensity of expression and number of SHIP-1 immunoreactive cells.

The progressive increase in SHIP-1 immunoreactivity found in the spinal cord of mSDO-1 mice, may reflect the progressive damage and loss of motor neurons associated with, at least in part, the inflammatory response. Downstream of PI3-kinase, PKB is largely involved in the regulation of cell

survival, cell proliferation and cell growth, and immunoreactivity of both kinases have been found to decrease at the early stages of ALS, when compared to age-matched wild-type tissue, prior to any significant loss of motoneurons (Warita et al., 2001). As previously mentioned, although the role of inflammation in ALS is not fully understood, it is known that excessive production of pro-inflammatory molecules can lead to collateral tissue damage (van Rossum et al., 2004). Furthermore, the significant increase in SHIP-1 immunoreactivity noted at end-stage in the mSOD-1 model, could contribute to decreased PI3-kinase expression, and may represent impairment in signaling pathways related to neuronal survival against apoptosis in ALS.

5.2 Heterogeneous expression of SHIP-1 in the spinal cord of mSOD-1 mice

The antibody used for these studies is directed to the N-terminus of SHIP-1, which is responsible for recruitment to the plasma membrane. Interestingly, the distribution of SHIP-1 immunoreactivity demonstrated regional differences where SHIP-1 immunoreactivity was most prominent in the most ventral regions of the ventral horn. Regional differences in SHIP-1 labelling were particularly obvious at the 15-week time-point. With evaluation of end-stage mSOD-1 tissue, the distribution of SHIP-1 became more homogeneous throughout the grey matter, as SHIP-1 labelling increased in both the ventral and dorsal horn regions.

This distribution of SHIP-1 immunoreactivty in mSOD-1 is similar to that previously reported with the cytoskeleton-associated protein, phospho-adducin (Shan et al., 2005) in mSOD-1 tissue, where there is prominent SHIP

immunoreactivity on the ventral-most aspect of the ventral horn. Additionally, from a molecular standpoint, assessment of spinal motoneurons from mouse models of ALS have shown PI3-kinase and PKB immunoreactivity to be greatest in the ventral region of the spinal cord (Warita et al., 2001), and because SHIP-1 negatively regulates expression levels of PtdIns (3,4,5)P3, the major player of PI3-kinase signaling, increased SHIP-1 labelling may coincide with regional differences in PI3-kinase activity. This pattern of immunoreactivity also reflects the pathology observed in mSOD-1 mice, where motoneurons lying within the ventral grey matter are progressively lost (Gurney et al., 1994). The basis for the motoneuron loss is unclear and there is also evidence for loss of other neuron types in mSOD-1 mice, including interneurons (Chang and Martin, 2009).

5.3 SHIP-1 immunoreactivity was not detected in microglia

In addition to changes in neuron numbers in mSOD-1 mice, there is considerable evidence for changes to the numbers and activation of astrocytes and microglia. Quantitative analysis has shown that in the mSOD-1 mouse studied here, that there are significant increases in the numbers of microglia in spinal cord tissue at cervical and lumbar spinal cord in mSOD-1 mice during disease progression (Hall et al., 1998). Furthermore, there is an increase in the number of activated astrocytes as determined using immunoreactivity to GFAP, a label for astrocyte-specific intermediate filaments, in mSOD-1 mice compared to age-matched wild-type mice (Hall et al., 1998). Given the presence of immunoreactivity to SHIP-1 in the spinal cord tissue from mSOD-1 mice, I initially hypothesized that this immunoreactivity would reflect an increase in the numbers

of microglia in mSOD-1 tissue. Microglia are tissue resident immune cells of the monocytic lineage and consequently it is not unexpected for this cell type to express monocytic markers. SHIP-1 immunoreactivity has been previously observed in lymphoid cells, such as B-cells, and myeloid cells, such as monocytes, tissue macrophages and mast cells; all of which are hematopoietic cells (Liu et al., 1998). On the other hand, previous research has not investigated SHIP-1 immunoreactivity in microglia using immunofluorescence techniques, and by double labelling spinal cord with antibody directed against SHIP-1, and either CD11b or Iba-1 antibodies which are markers for microglia, interestingly, I found that SHIP-1 immunoreactivity did not co-localize with Iba-1 or CD11b, indicating that detectable SHIP-1 immunoreactivity was not present in microglia.

Astrocytes represent a large population of cells in the CNS and by some accounts comprise more than 40% of all CNS cells. To explore the distribution of SHIP-1 further, GFAP was used as an astrocyte-specific marker. When spinal cord from mSOD-1 mice was double labelled with SHIP-1 and GFAP, SHIP-1 was found to co-localize with astrocytes, strongly suggesting that SHIP-1 immunoreactivity is present in some astrocytes in mSOD-1 mice. There is no previous report on SHIP-1 expression in astrocytes, and previous reports looking at the immunoreactivity of SHIP-1 in other cell lineages report conflicting results. For example, using immunohistochemical labelling techniques, SHIP-1 was previously detected in embryonic cells giving rise to both hematopoietic and endothelial cells (Liu et al., 1998). However, in later stages of embryo development, SHIP-1 immunoreactivity was only detected in cells differentiating

from the mesoderm (Liu et al., 1998). In contrast to this finding, in a recent study that assessed the immunoreactivity of SHIP in CNS, a commercial goat polyclonal anti-SHIP1 antibody was used to examine rat hypothalamic tissue (Bertelli et al., 2006). The authors found that SHIP-1 immunolabelling was distributed in cells having insulin receptor immunoreactivity, which were interpreted as being neurons. Also, in this study hypothalamic total protein extracts were blotted and examined with anti-SHIP-1 antibodies. Bands corresponding to approximately 50 kDa and 70 kDa were found, considerably less than the approximate 150 kDa band expected for full length SHIP-1. The authors claimed that although only a faint band was observed at approximately 150 kDa, which potentially might also have been SHIP-2, the more prominent bands at 50 kDa and 70 kDa were shown to be due to a protein that underwent tyrosine phosphorylation by insulin and was identified as being a 5'phosphatase-IV protein, which shares sequence homology with SHIP-1 and SHIP-2 (32% similarity with SHIP-1; Bertelli et al., 2006). Thus, whether SHIP-1 immunoreactivity that is independent of 5'phosphatase immunoreactivity is present in hypothalamus, or other brain region, remains unknown. However, the authors of this study did find a faint 150 kDa band in hypothalamus using Western blotting with anti-SHIP1 antibodies, suggesting there is at least some SHIP-1 protein in rat hypothalamus. This was reported to be much less than in rat thymic tissue (Bertelli et al., 2006).

5.4 Morphological phenotype of SHIP-1 immunoreactive cells

In addition to the evaluating the cell-type of SHIP-1 expressing cells by immunoreacitivity to markers for microglia and astrocytes, the morphological features of the SHIP-1 labelled cells were assessed. Some SHIP-1 immunoreactive cells appeared stellate-shaped and possessed small cell bodies and very long, narrow processes, while others appeared polygonal, had thickened or more rounded shaped cell bodies, and possessed short ramifications. Not all cells immunoreactive for GFAP co-expressed SHIP-1; however, it appeared as though all SHIP-1 immunoreactive cells were co-labelled with GFAP in the end-stage mSOD-1 mice. Cells that were immunoreactive for both SHIP-1 and GFAP exhibited the larger and more rounded cell body phenotype and this is consistent with the morphology of activated astrocytes found during periods of inflammation. Microglia labelled with either Iba-1 or CD11b also exhibited phenotypical characteristics of activated glia, despite failing to co-label with SHIP-1 immunoreactive cells.

5.5 Conclusions

While SHIP-1 is expressed at very low levels in un-stimulated cells, its rapid up-regulation and recruitment to the plasma membrane following PI3-kinase phosphorylation has been previously reported in tissue macrophages involved in the pro-inflammatory response (Parsa et al., 2006; Sly et al., 2003; Sly et al., 2004). The action of recruitment to the plasma membrane coincides with the observations made in this study, where increased immunoreactivity of SHIP-1 in

the spinal cord was detected in mSOD-1 expressing mice, but not in wild-type mice.

One reason why SHIP-1 was not found to be not expressed in microglia could be explained if the microglia in the mSOD-1 spinal cord tissue were alternatively activated, or expressing a phenotype characteristic of healing or anti-inflammatory cells. Previous research has indicated that SHIP-1 deficient cells, particularly macrophages, become skewed towards an alternative phenotype (Rauh et al., 2005). While this hypothesis seems viable given the current position on SHIP-1 expression and its role in dampening the pro-inflammatory process, this suggestion is not supported by previous research relating to ALS. In mSOD-1 models of ALS, it has been suggested that microglia may exacerbate the inflammatory response and degenerative process of neurons through the secretion of pro-inflammatory molecules (Kuhle et al., 2009).

A second possible explanation for the restricted expression of SHIP-1 may relate to the expression of PI3-kinase. Significant differences in the levels of immunoreactivity of PI3-kinase and PKB, between anterior horn neurons and glia cells, have been reported in mSOD-1 mice (Warita et al., 2001). Moreover, while immunoreactiivty has been found to decrease with disease progression in motoneurons, expression in glia cells has been described as infrequent or mild, at all stages of disease (Warita et al., 2001). Should PI3-kinase and PKB expression be limited in microglia cells, the level of SHIP-1 immoreactivity may go undetected with immunohistochemical techniques.

In the current study, spinal cord tissue from a SHIP-1$^{-/-}$ mouse was used as a negative control, and when immunohistochemistry was performed using the antibody directed against SHIP-1, no specific immunoreactivity was detected. Therefore, it is unlikely that the specific immunoreactivity detected in mSOD-1 tissue was not specific to SHIP-1. On the other hand, a BLAST search of the protein could be performed to detect any problems with the antibodies or antigenic sites given that only one of the antibodies resulted in immunofluorescence staining. SHIP-1 immunoreactivity was visible around the peripheral regions of white matter in some tissue sections, which appeared to be most intense in mSOD-1 spinal cord sections. The presence of SHIP-1 staining in regions of white matter clearly contradicts previous, with the exception of the observations made by Bertelli et al. (2006). However, should the phosphatase SHIP-2 have been detected, then in accordance with previous findings, SHIP-2 immunoreactivity would also have been expected to be found in microglia.

In conclusion, these data do not allow me to positively affirm whether the changes in SHIP-1 immunoreactivity are a cause or consequence of disease in the mSOD-1 mouse. However, given that the mSOD-1 mouse model of ALS is characterized by mutations in superoxide dismutase, it seems unlikely that a major effect of these SOD mutations would be to act selectively on either the SHIP-1 protein level, or SHIP-1 enzyme activity. Consequently, I suspect that the change in SHIP-1 immunoreactivity I observed in the mSOD-1 spinal cord tissue reflects an up-regulation of SHIP-1 protein during disease that may be either compensatory or a consequence of the disease process in the mSOD-1 mouse.

5.6 Future research

Similar to tissue macrophages, LPS can activate microglial cells, resulting in the production of a wide range of pro-inflammatory factor such TNF-α (Zhao et al., 2004) LPS can also induce the production of NO by microglial cells, which is a common characteristic of microglia in ALS. Previous research has reported SHIP-1 expression and activity at the plasma membrane to increase significantly, in response to the LPS-induced pro-inflammatory response or the innate immune response in induced pro-inflammatory infections (Parsa et al., 2006). To further evaluate the expression of SHIP-1 in spinal cord tissue, a pro-inflammatory response induced by LPS or through the use of an experimental autoimmune encephalitis (EAE) mouse model of multiple sclerosis (MS), could used to evaluate the immunoreactivity of SHIP-1. Double-labelling techniques could then be employed to study the cell-specific changes in SHIP-1 expression in an environment conducive to the pro-inflammatory response, eliminating any ambiguity associated with the inflammatory state in the mSOD-1 model.

Performing *ex vivo* cell specific immunoreactive assessments of astrocytes and microglia, following the use of cell sorting and cell purification techniques, could also be a viable method to test for the expression of SHIP-1 in both types of glia cells. This procedure could be carried out using spinal cord tissue of mSOD-1 mice to identify the expression of SHIP-1 in the mSOD-1 model and to characterize the inflammatory state of glia cells in SHIP-1 expressing tissue.

6: APPENDICES

6.1 Appendix A: Immunohistochemistry protocol

6.1.1 OCT mounting

1. Apply a small amount of Optimal Cutting Temperature Medium (OCT) to metal surface of cryostat stage, in the shape of a circle, to serve as the base of a mold.
2. Once the OCT Medium starts to set, or solidify, carefully place the caudal end of the spinal cord into the medium.
3. Carefully hold the spinal cord in an upright position until it freezes in place.
4. Once the OCT has set and the spinal cord remains in place, cover the area of the spinal cord with a small amount of OCT, and repeat this several times, in order to build-up a protective covering over the spinal cord.
5. Once the final application has set, and the spinal cord is fully covered, remove the spinal cord from the metal working surface and wrap it in parafilm, and label it appropriately for future identification
6. The spinal cord should then be stored indefinitely at -80°C until it is ready to be cut.

6.1.2 Cryosectioning

1. Set the temperature for the cryostat block to 15-17°C, and the box temperature to -23 °C.

2. Set the section thickness adjustment to read 30um.

3. Use a small amount of OCT medium to mount the spinal cord section onto the stage and if necessary, use a razor blade to remove excess mounting to allow for proper alignment of the tissue on the mounting block.

4. Place the stage in the holder, align with the cryostat blade, and secure the stage. Again, if necessary, use a razor blade to trim away excess OCT sample.

5. Prepare the appropriate number of autoclaved 1.5ml eppendorf tubes that will be needed for the tissue sections, and fill each tube ¾ full with de Olomos solution.

6. Turn on the cryostat and begin slicing, and collect every 5th tissue section.

7. Sections placed in de Olomos1 solution should be stored at -20°C until needed.

6.1.3 Immunohistochemical staining

6.1.3.1 Solutions

0.3 % PBST (500 ml)
1. 473. ml ddH20
2. 25 ml 20x Phosphate Buffered Saline
3. 1.5 ml Triton–X

Blocking Solution (4mll)
1. 2.88 ml of PBST
2. 1 ml Natural Donkey Serum (25 % NDS)
3. 0.12 g Bovine Serum Albumin (3 % BSA)

Primary Antibody Solution (4 ml)
1. 3.48 ml PBST
2. 400 ul Normal Donkey Serum (10 % NDS)
3. 0.12 g Bovine Serum Albumin (3 % BSA)
4. Add primary antibody according to optimal dilution
    a. SHIP-1 (Stemcell)- 1:1000, where 3 ml of solution requires 3 ul of antibody
    b. Iba-1- 1:1000
    c. CD11b- 1:500
    d. GFAP- 1:200

Secondary Antibody Solution (4 ml)
1. 3.48 ml PBST
2. 400 ul Normal Donkey Serum (10 % NDS)
3. 0.12 g Bovine Serum Albumin (3 % BSA)
4. Add Secondary Antibody according to optimal dilution
    a. Cy3- 1:1000, where 3 ml of solution requires 3 ul of antibody
    b. Alexa647- 1:1000
    c. FITC- 1:1000

6.1.3.2 Staining procedure

1. Rise sections 3 x 10 s followed by 3 x 15 m in PBST in well tissue culture plate on shaker.
2. Remove sections from PBST and place into 0.5 M Glycine solution for antigen retrieval, for 1 h at room temperature
3. Rise sections 3 x 10 s followed by 3 x 5 m in PBST in well tissue culture plate on shaker.
4. Remove sections from Glycine solution and add 1.5 ml of Blocking solution to each well and incubate for 1 h at room temperature.
5. Remove Blocking solution and add 1.5 ml of Primary antibody solution (negative controls placed in solution without antibody).
6. Immediately cover tissue culture plate and place in fridge at 4°C for 24 h, or overnight.
7. Remove Primary antibody solution, and rinse sections for 3 x 10 s followed by 5 x 10 m in PBST in well tissue culture plate on shaker.
8. Incubate in Secondary antibody solution for 2 h at room temperature on shaker. Culture plate must be covered with foil for the duration of the experiment because the antibody is light sensitive.
9. Rise sections 3 x 10 s followed by 5 x 10 m in PBST in well tissue culture plate on shaker.
10. Slide mount tissue sections with a fine-tipped paint brush and allow the sections to dry
11. Add a small drop of Vectashield Mounting Medium to the centre of each slide, and slowly lower a cover slip over the Mounting Medium while avoiding any bubbles between the slide and cover slip.
12. Let the cover slip sit for 5 min to ensure the Vectashield Mounting Medium has spread evenly under the cover slip, and then adhere the cover slip to the slide using clear nail polish.
13. After the nail polish dries, store indefinitely at 4°C

REFERENCE LIST

Alexianu ME, Kozovska M, and Appel SH. (2001) Immune reactivity in a mouse model of familial ALS correlates with disease progression. *Neurology,* 57: 1282-1290.

Aloisi F. (2001) Immune function of microglia. *Glia* 36: 165–179.

Aman MJ, Lamkin TD, Okada H, Kurosaki T and Ravichandran S. (1998) The inositol phosphatase SHIP inhibits Akt/PKB activation in B cells. *Journal of Biological Chemistry*. 273: 33922-33928.

Aman MJ, Walk SF, March ME, Su HP, Carver DJ, and Ravichandran KS. (2000) Essential role for the C-terminal noncatalytic region of SHIP in FcgammaRIIB1-mediated inhibitory signaling. *Molecular and Cellular Biology*, 20: 3576-3589.

Barron KD. (1995) The microglial cell. A historical review. *Journal of Neurological Science,* 134: 57-68.

Bertelli DF, Araújo EP, Cesquini M, Stoppa GR, Gasparotto-Contessotto M, Toyama MH, et al. (2006) Phosphoinositide-specific inositol polyphosphate 5-phosphatase IV inhibits inositide trisphosphate accumulation in hypothalamus and regulates food intake and body weight. *Endocrinology,* 147(11): 5385-99.

Brauweiler A, Tamir I, Marschner S, Helgason CD, and Cambier JC. (2001) Partially distinct molecular mechanisms mediate inhibitory FcyRIIB signaling in resting and activaged B cells. *Journal of Immunology*, 167: 204-211.

Bruijn LI, Miller TI, and Cleveland DW. (2004) Unraveling the mechanisms involved in motor neuron degeneration in ALS*. Annual Review of Neuroscience,* 27: 723-749.

Brunori M. and Rotilio G. (1984) Biochemistry of oxygen radical species. *Methods in Enzymology*, 105: 22-35.

Brunet A, Bonni A, Zigmond MJ, Lin MZ, Juo P, Hu LS, et al. (1999) Akt promotes cell survival by phosphorylating and inhibiting a Forkhead transcription factor. *Cell,* 96: 857-868.

Camps M, Ruckle T, Ji H, Ardissone V, Rintelen F, Shaw J, et al. (2005) Blockade of PI3K suppresses joint inflammation and damage in mouse models of rheumatoid arthritis. *Nature Medicine,* 11: 936– 943.

Cantley LC. (2002) The phosphoinositide 3-kinase pathway. *Science,* 296: 1655-1657.

Cardone MH, Roy N, Stennicke HR, Salvesen GS, Franke TF, Stanbridge E, et al. (1998) Regulation of cell death protease caspase-9 by phosphorylation. *Science,* 282(5392): 1318-1321.

Chacko GW, Tridandapani S, Damen JE, Liu L, Krystal G, and Coggeshall KM. (1996) Negative signaling in B-lymphocytes induces tyrosine phosphorylation of the 145-kDa inositol polyphosphate 5-phosphatase, SHIP. *Journal of Immunology,* 157: 2234-2238.

Chang Q, and Martin LJ. (2009). Glycinergic innervation of motoneurons is deficient in amyotrophic lateral sclerosis mice: a quantitative confocal analysis. *The American Journal of Pathology,* 174(2): 574-85.

Chiu AY, Zhai P, Dal Canto MC, Peteres TM, Kwon YW, Prattis SM, and Gurney ME. (1995) Age-dependent penetrance of disease in a transgenic mouse model of familial amyotrophic lateral sclerosis. *Molecular and Cellular Neuroscience,* 6: 349-362.

Coggeshall KM. (1998) Inhibitory signaling by B cell Fc gamma RIIb. *Current Opinion in Immunology,* 10(3): 306-12.

Cunningham LR. (2005) Increased skeletal muscle akt content in a murine model of motor neuron disease. Master's thesis, Simon Fraser University, Burnaby, British Columbia.

Damen JE, Liu L, Rosten P, Humphries RK, Jefferson AB, Majerus PW, et al. (1996) The 145-kDa protein induced to associate with Shc by multiple cytokines is an inositol tetraphosphate and phosphatidylinositol 3,4,5-trisphosphate 5-phosphatase. *Proceedings of the National Academy of Sciences,* 93: 1689–1693.

Damen J E, Ware MD, Kalesnikoff J, Hughes MR, and Krystal G. (2001) SHIP's C-terminus is essential for its hydrolysis of PIP3 and inhibition of mast cell degranulation. *Blood,* 97:1343-1351.

Dennis PB, Jaeschke A, Saitoh M, Fowler B, Kozma SC, and Thomas G. (2001) Mammalian TOR: a homeostatic ATP sensor. *Science*, 294(5544): 1102-1105.

Dudek H, Datta SR, Franke TF, Birnbaum MJ, Yao R, Cooper RM, et al. (1997) Regulation of neuronal survival by the serine-threonine protein kinase Akt. *Science,* 275: 661-664.

Eisen A, and Krieger C. (1998) Amyotrophic lateral sclerosis: A synthesis of research and clinical practice. Cambridge, UK: University Press.

Engleman JA, Luo J, and Cantley LC. (2006) The evolution of phosphatidylinositol 3-kinases as regulators of growth and metabolism. *Nature Reviews Genetics*, 7(8): 606-619.

Fruman DA, Meyers RE, and Cantley LC. (1998) Phosphoinositide kinases. *Annual Review of Biochemistry* 67: 481-507.

Geier SJ, Algate PA, Carlberg K, Flowers D, Friedman C, Trask B, et al. (1997) The human SHIP gene is differentially expressed in cell lineages of the bone Marrow and Blood. *Blood,* 89: 1876-1885.

Gingras AC, Raught B, and Sonenberg N. (2001) Regulation of translation initiation by FRAP/mTOR. *Genes and Development,* 15(7): 807-826.

Gloire G, Erneux C, and Piette J. (2007) The role of SHIP1 in T-lymphocyte life and death. *Biochemical Society Transactions,* 35(2): 277-280.

Guegan C, and Przedborski S. (2003) Programmed cell death in amyotrophic lateral sclerosis. *Journal of Clinical Investigation*, 111: 153-161.

Gurney ME, Pu H, Chiu AY, Dal Canto MC, Polchow CY, Alexander DD, et al. (1994) Motor neuron degeneration in mice that express a human Cu,Zn superoxide dismutase mutation. *Science,* 264: 1772-1775.

Hall ED, Oostveen JA, and Gurney ME. (1998) Relationship of microglial and astrocytic activation to disease onset and progression in a transgenic model of familial ALS, *Glia* 23: 249-256.

Hawkins PT, Anderson KE, Davidson K, and Stephens LR. (2006) Signaling through class I PI3Ks in mammalian cells. *Biochemical Society Transactions,* 34: 647-662.

Helgason C, Damen J, Rosten P, Grewal R, Sorensen P, Chappel S, et al. (1998) Targeted disruption of SHIP leads to hemopoietic perturbations, lung pathology,and a shortened life span. *Genes and Development,* 12(11): 1610-1620.

Horn S, Endl E, Fehse B, Weck MM, Mayr GW, and Jucker M. (2004) Restoration of SHIP activity in a human leukemia cell line downregulates constitutively activated phosphatidylinositol 3-kinase/Akt/Gsk-3beta signaling and leads to an increased transit time through the G1 phase of the cell cycle. *Leukemia,* 18: 1839-1849.

Hu JH. (2003). Abnormal protein phosphorylation in human amyotrophic lateral sclerosis. Unpublished master's thesis, Simon Fraser University, Burnaby, British Columbia.

Hu J, Chernoff K, Pelech S, and Krieger C. (2003) Protein kinase and protein phosphatase expression in the central nervous system of G93A SOD over-expressing mice. *Journal of Neurochemistry,* 85: 422-431.

Huber M, Helgason CD, Damen JE, Liu L, Humphries RK, and Krystal, G. (1998) The src homology 2-containing inositol phosphatase (SHIP) is the gatekeeper of mast cell degranulation. *Proceedings of the National Academy of Sciences,* 95: 11330-11335.

Huber M, Helgason CD, Damen JE, Scheid M, Duronio V, Liu L, et al. (1999) The role of SHIP in growth factor induced signalling. *Progress in Biophysics and Molecular Biology*, 71: 423-434.

Julien JP. (2001) Amyotropic lateral sclerosis. Unfolding the toxicity of the misfolded. *Cell,* 104: 581-591.

Kandel E. (2000) Nerve cells and behavior. In Kandel E, Schwartz JH, Jessell TM (Eds.), *Principles of Neural Science* (4th ed.) New York, NY: McGraw-Hill Professional Publishing. pp 20.

Kapeller R, and Cantley LC. (1994) Phosphatidylinositol 3-kinase. *Bioessays,* 16: 565–576.

Katso R, Okkenhaug K, Ahmadi K, White S, Timms J, and Waterfield MD. Cellular function of phosphoinositide 3-kinases: implications for development, homeostasis, and cancer. (2001) *Annual Review of Cell and Developmental Biology,* 17: 615-675.

Kawamata T, Akiyama H, Yamada T, McGreer PL. (1992) Immunologic reactions in amyotrophic lateral sclerosis brain and spinal cord tissue. *American Journal of Pathology*, 140: 691-707.

Kim CH, Hangoc G, Cooper S, Helgason CD, Yew S, Humphries RK, et al. (1999) Altered responsiveness to chemokines due to targeted disruption of SHIP. *The Journal of Clinical Investigation*, 104(12): 1751–1759.

Kreutzberg GW. (1996) Microglia: a sensor for pathological events in the CNS. *Trends in Neurosciences,* 19(8): 312-318.

Krieger C, Lanius RA, Pelech SL, and Shaw CA. (1996) Amyotrophic lateral sclerosis: the involvement of intracellular CA^{2+} and protein kinase C. *Trends in Pharmacological Sciences,* 17: 114-120.

Krystal G, Damen JE, Helgason CD, Huber M, Hughes MR, Kalesnikoff J, et al. (1999) SHIPs ahoy. *International Journal of Biochemistry and Cell Biology*, 10: 1007-1010.

Kuhle J, Lindberg RLP, Regeniter A, Mehling M, Steck AJ, Kappos L, et al. (2009) Increased levels of inflammatory chemokines in amyotrophic lateral sclerosis. *European Journal of Neurology,* 16(6): 771-774.

Li N, Batzer A, Daly R, Yajnik V, Skolnik E, Chardin P, Bar-Sagi D, Margolis B, and Schlessinger J. (1993) Guanine-nucleotide releasing factor hSosl binds to Grb-2 and links tyrosine kinases to Ras signalling. *Nature*, 363: 85-87.

Liu Q, Sasaki T, Kozieradzki I, Wakeham A, Itie A, Dumont DJ, et al. (1999) SHIP is a negative regulator of growth factor receptor-mediated PKB/Akt activation and myeloid cell survival. *Genes and Development,* 13(7): 786-791.

Liu Q, Shalaby F, Jones J, Bouchard D, Dumont DJ. (1998) The SH2 containing inositol polyphosphate 5-phosphatase, SHIP, is expressed during hematopoiesis and spermatogenesis. *Blood*, 91: 2753-2759.

Luo JM, Yoshida H, Komura S, Ohishi N, Pan L, Shigeno K, et al. (2003) Possible dominant-negative mutation of the SHIP gene in acute myeloid leukemia. *Leukemia* ,17: 1-8.

March ME, and Ravichandran K. (2002) Regulation of the immune response by SHIP. *Seminars in Immunology,* 14(1): 37-47.

McCord J.M. and Fridovich I. (1969) The utility of superoxide dismutase in studying free radical reactions. I. Radicals generated by the interaction of sulfite, dimethyl sulfoxide, and oxygen. *Journal of Biological Chemistry*, 244:6056-6063,

Muraille E, Pesesse X, Kuntz C, and Erneu, C. (1999) Distribution of the src-homology-2-domain-containing inositol 5-phosphatase SHIP-2 in both non-haemopoietic and haemopoietic cells and possible involvement of SHIP-2 in negative signalling of B-cells. *Biochemical Journal*, 342(3): 697-705.

Nimmerjahn A, Kirchoff F, Helmchen F. (2005) Resting microglia cells are highly dynamic surveillants of brain parenchyma in vivo. *Science,* 308 (5726): 1314-1318.

Olson MF, and Marais R. (2000) Ras protein signaling. *Seminars in Immunology*, 12: 63-73.

Paez J, Sellers WR (2003) PI3K/PTEN/AKT pathway. A critical mediator of oncogenic signaling. *Cancer Treatment Research*, 115: 145–167.

Parsa KV, Ganesan LP, Rajaram MV, Gavrilin MA, Balagopal A, Mohapatra NP, et al. (2006) Macrophage Pro-inflammatory response to francisella novicida infection is regulated by SHIP. *PLoS Pathogens,* 2(e71): 0681-0690.

Pesesse X, Deleu S, De Smedt F, Drayer L, and Erneux C. (1997) Identification of a second SH2-domain-containing protein closely related to the phosphatidylinositol polyphosphate 5-phosphatase SHIP. *Biochemical and Biophysical Research Communications,* 239: 697-700.

Rauh MJ, Kalesnikoff J, Hughes M, Sly L, Lam V, and Krystal, G. (2003) Role of Src homology 2-containing-inositol 5'-phosphatase (SHIP) in mast cells and macrophages. *Biochemical Society Transactions,* 31: 286-291.

Rauh MJ, Ho V, Pereira C, Sham S, Sly LM, Lam V, et al. (2005) SHIP represses the generation of alternatively activated macrophages. *Immunity*, 23: 361–74.

Reaume AG, Elliott JL, Hoffman EK, Kowall NW, Ferrante RJ, Siwek DF, et al. (1996) Motor neurons in Cu/Zn superoxide dismutase-deficient mice develop normally but exhibit enhanced cell death after axonal injury. *Nature Genetics*, 13: 43-47.

Rohrschneider LR, Fuller JF, Wolf I, and Liu Y, Lucas DM. (2000) Structure, function, and biology of SHIP proteins. *Genes and Development,* 14(5): 505-520.

Rosen DR, Siddique T, Patterson D, Figlewicz DA, Sapp P, Hentati A, et al. (1993) Mutations in Cu/Zn superoxide dismutase gene are associated with familial amyotrophic lateral sclerosis. *Nature*, 362: 59–62.

Sargsyan SA, Monk PN, Shaw PJ. (2005) Microglia as potential contributors to motor neuron injury in amyotropic lateral sclerosis. *Glia,* 51:241-253.

Sedgwick JD, Hickey WF. (1997) Antigen presentation in the nervous system. In Keane RW, Hickey WF (Eds.), *Immunology of the nervous system* New York: Oxford University Press. pp 364–418.

Sly LM, Ho V, Antignano F, Ruschmann J, Hamilton M, Lam V, Rauh MJ, Krystal G. (2007) The role of SHIP in macrophages. *Frontiers in Bioscience,* 12: 2836-2848.

Sly LM, Rauh MJ, Kalesnikoff J, Buchse T, and Krystal G. (2003) SHIP, SHIP2, and PTEN activities are regulated in vivo by modulation of their protein levels: SHIP is up-regulated in macrophages and mast cells by lipopolysaccharide. *Experimental Hematology,* 31(12): 1170-81.

Sly LM, Rauh MJ, Kalesnikoff J, Song CH, and Krystal G. (2004) LPS-induced upregulation of SHIP is essential for endotoxin tolerance. *Immunity*, 21: 227-239.

Stein M, Keshav S, Harris N, Gordon S. (1992) Interleukin 4 potently enhances murine macrophage mannose receptor activity: a marker of alternative immunologic macrophage activation. T*he Journal of Experimental Medicine,* 176(1): 287–292.

Stein RC, and Waterfield MD. (2000) PI 3-kinase inhibition: a target for drug development? *Molecular Medicine Today*, 6(9): 347 -357.

Stephens L, McGregor A, and Hawkins P. (2000) Phosphoinositide 3-kinases: regulation by cell-surface receptors and function of 3-phosphorylated lipids. In S. Cockcroft (Ed.), Biology of phosphoinositides (pp. 32–130). Oxford: Oxford University Press.

Stoll G, Jander S and Schroeter, M. (2002) Detrimental and beneficial effects of injury-induced inflammation and cytokine expression in the nervous system. *Advances in Experimental Medicine and Biology*, 513: 87-113

Strong JM, Kesavapany S, and Pant HC. (2005) The pathobiology of amyotrophic lateral sclerosis: a proteinopathy? *Journal of Neuropathology and Experimental Neurology,* 64(8): 649-62.

Toker AM, Meyer M, Reddy KK, Falck JR, Aneja R, Aneja S, et al. (1994) Activation of protein kinase C family members by the novel polyphosphoinositides PtdIns-3,4-P_2 and PtdIns-3,4,5-P_3. *Journal of Biological Chemistry*, 269: 32358–32367.

Tridandapani S, Chacko GW, Van Brocklyn JR, and Coggeshall KM. (1997a) Negative signaling in B cells causes reduced Ras activity by reducing Shc-Grb2 interactions. *Journal of Immunology,* 158: 1125-1132.

Tridandapani S, Kelly T, Cooney D, Pradhan M, Coggeshall KM. (1997b) Negative signaling in B cells: SHIP Grbs Shc. *Immunology Today,* 18: 424-427.

Vanhaesebroeck B, Leevers SJ, Ahmadi K, Timms J, Katso R, Driscoll PC, et al. (2001) Synthesis and function of 3-phosphorylated inositol lipids. *Annual Review of Biochemistry*, 70: 535-602.

Vanhaesebroeck B, and Waterfield MD. (1999) Signaling by distinct classes of phosphoinositide 3-kinases. *Experimental Cell Research*, 253(1): 239–254.

van Rossum D, Hanisch UK. (2004) Microglia. *Metabolic Brain Disease,* 19: 393–411.

Viatour P, Merville MP, Bours V, and Chariot A. (2005) Phosphorylation of NF-κB and IκB proteins: implications in cancer and inflammation. *Trends in Biochemical Sciences*, 30(1): 43-52.

Vilhardt F (2005) Microglia: phagocyte and glia cell. *International Journal of Biochemistry and Cell Biology* 37:17–21.

Vivanco I, and Sawyers CL. (2002) The phosphatidylinositol 3-Kinase-AKT pathway in human cancer. *Nature Reviews Cancer*, 2: 489–501.

Wagey R, Pelech SL, Duronio V, and Krieger C. (1998) Phosphatidylinositol 3-kinase: Increased activity and protein level in amyotrophic lateral sclerosis. *Journal of Neurochemistry,* 71: 716–722.

Ware MD, Rosten P, Damen JE, Liu L, Humphries RK, and Krystal G. (1996) Cloning and characterization of human SHIP, the 145-kD inositol 5-phosphatase that associates with SHC after cytokine stimulation. *Blood*, 88: 2833–2840.

Warita H, Manabe Y, Murakami T, Shiro Y, Nagano I, and Abe K. (2001) Early decrease of survival signal-related proteins in spinal motor neurons of presymptomatic transgenic mice with a mutant SOD1 gene. *Apoptosis*, 6: 345–352.

Wiedau-Pazos M, Goto JJ, Rabizadeh S, Gralla EB, Roe JA, Lee MK, Valentine JS, and Bredesen DE. (1996) Altered reactivity of superoxide dismutase in familial amyotrophic lateral sclerosis. *Science*, 271: 515-518.

Wootz, H. (2006) Amyotrophic lateral sclerosis- a study in transgenic mice. in: Digital Comprehensive Summaries of Uppsala Dissertations from the Faculty of Medicine 250. Acta Universitatis Upsaliensis, Uppsala, Sweden.

Wymann M, and Pirola L. (1998) Structure and function of phosphoinositide 3-kinases. *Biochimica et Biophysica Acta-Molecular and Cell Biology of Lipids,* 1436: 127-150.

Xiao Q, Zhao W, Beers D, Yen D, Xie W, Henkel JS, et al. (2007) Mutant SOD1G93A microglia are more neurotoxic relative to wild-type microglia. *Journal of Neurochemistry*, 102: 2008-2019.

Yim MB, Kang JH, Yim HS, Kwak HS, Chock PB, and Stadtman ER. (1996) A gain-of-function of an amyotrophic lateral scerosis-associated Cu,Zn-superoxide dismutase mutant: An enhancement of free radical formation due to a decrease in Km for hydrogen peroxide. *Proceedings of the National Academy of Sciences USA*, 93: 5709-5714.

Zhao W, Xie W, Le W, Beers DR, He Y, Henkel JS, Simpson EP, et al. (2004) Activated microglia initiate motor neuron injury by a nitric oxide and glutamate-mediated mechanism, *Journal of Neuropathology & Experimental Neurology,* 63: 964–977.